2013-03

Refractive conditions of Amazon environment and its effects on ground and airborne radar and ESM systems

Ferrari, Jair Feldens

Monterey, California. Naval Postgraduate School

NAVAL
POSTGRADUATE
SCHOOL

MONTEREY, CALIFORNIA

THESIS

REFRACTIVE CONDITIONS OF AMAZON ENVIRONMENT AND ITS EFFECTS ON GROUND AND AIRBORNE RADAR AND ESM SYSTEMS

by

Jair Feldens Ferrari

September 2003

Thesis Advisor:	Kenneth L. Davidson
Co-Advisor:	David C. Jenn

Approved for public release; distribution is unlimited

THIS PAGE INTENTIONALLY LEFT BLANK

REPORT DOCUMENTATION PAGE			Form Approved OMB No. 0704-0188
Public reporting burden for this collection of information is estimated to average 1 hour per response, including the time for reviewing instruction, searching existing data sources, gathering and maintaining the data needed, and completing and reviewing the collection of information. Send comments regarding this burden estimate or any other aspect of this collection of information, including suggestions for reducing this burden, to Washington headquarters Services, Directorate for Information Operations and Reports, 1215 Jefferson Davis Highway, Suite 1204, Arlington, VA 22202-4302, and to the Office of Management and Budget, Paperwork Reduction Project (0704-0188) Washington DC 20503.			
1. AGENCY USE ONLY *(Leave blank)*	**2. REPORT DATE** September 2003	**3. REPORT TYPE AND DATES COVERED** Master's Thesis	
4. TITLE AND SUBTITLE: Refractive Conditions of Amazon Environment and Its Effects on Ground and Airborne Radar and ESM Systems			**5. FUNDING NUMBERS**
6. AUTHOR(S) Ferrari, Jair F.			
7. PERFORMING ORGANIZATION NAME(S) AND ADDRESS(ES) Naval Postgraduate School Monterey, CA 93943-5000			**8. PERFORMING ORGANIZATION REPORT NUMBER**
9. SPONSORING /MONITORING AGENCY NAME(S) AND ADDRESS(ES) N/A			**10. SPONSORING/MONITORING AGENCY REPORT NUMBER**
11. SUPPLEMENTARY NOTES The views expressed in this thesis are those of the author and do not reflect the official policy or position of the Department of Defense or the U.S. Government.			
12a. DISTRIBUTION / AVAILABILITY STATEMENT Approved for public release; distribution is unlimited.			**12b. DISTRIBUTION CODE**

13. ABSTRACT (maximum 200 words)

This is a study of abnormal refractive layer occurrence over the Amazon region and possible effects on radar and ESM systems, ground or airborne based. Climatologic data from three stations in that region are analyzed using computations from the Global Tropospheric Experiment (GTE), soundings and satellite imagery. The GTE data provide monthly occurrences and seasonality of atmospheric ducts and superrefractive layers. Further, individual soundings from the March-June 2003 period and the Advanced Refractive Effects Prediction Systems (AREPS) 2.1 software are used in a case study that analyzed these layers and, in addition, subrefractive and multiple layers. Selected soundings were used in simulations to explain the effects of different types of abnormal layers on the electromagnetic propagation. Although abnormal layers did not affect ground systems, airborne ones were. For radar, a region with low or no detection is created when an abnormal layer refracts the electromagnetic energy upwards or downwards. Some combinations of multiple layers may cause effects even stronger. It is concluded that knowledge of the abnormal layers occurrence is important for operations in the Amazon region. Further, airborne radar platforms should measure local refractive conditions, if possible. A comprehensive study in time and space is recommended to provide forecasting.

14. SUBJECT TERMS Electronic warfare, electromagnetic propagation, Amazon, abnormal refractive layers, refractive conditions, climatologic data, AREPS, radar, ESM, atmospheric ducts, superrefraction, subrefraction.			**15. NUMBER OF PAGES** 89
			16. PRICE CODE
17. SECURITY CLASSIFICATION OF REPORT Unclassified	**18. SECURITY CLASSIFICATION OF THIS PAGE** Unclassified	**19. SECURITY CLASSIFICATION OF ABSTRACT** Unclassified	**20. LIMITATION OF ABSTRACT** UL

NSN 7540-01-280-5500 Standard Form 298 (Rev. 2-89)
Prescribed by ANSI Std. 239-18

THIS PAGE INTENTIONALLY LEFT BLANK

Approved for public release; distribution is unlimited

REFRACTIVE CONDITIONS OF AMAZON ENVIRONMENT AND ITS EFFECTS ON GROUND AND AIRBORNE RADAR AND ESM SYSTEMS

Jair Feldens Ferrari
Lieutenant Colonel, Brazilian Air Force
B.S., Brazilian Air Force Academy, 1984

Submitted in partial fulfillment of the
requirements for the degree of

MASTER OF SCIENCE IN SYSTEMS ENGINEERING

from the

NAVAL POSTGRADUATE SCHOOL
September 2003

Author: Jair Feldens Ferrari

Approved by: Kenneth L. Davidson
Thesis Advisor

David C. Jenn
Co-Advisor

Dan C. Boger
Chairman, Information Sciences Department

THIS PAGE INTENTIONALLY LEFT BLANK

ABSTRACT

This is a study of abnormal refractive layer occurrence over the Amazon region and possible effects on radar and ESM systems, ground or airborne based. Climatologic data from three stations in that region are analyzed using computations from the Global Tropospheric Experiment (GTE), soundings and satellite imagery. The GTE data provide monthly occurrences and seasonality of atmospheric ducts and superrefractive layers. Further, individual soundings from the March-June 2003 period and the Advanced Refractive Effects Prediction Systems (AREPS) 2.1 software are used in a case study that analyzed these layers and, in addition, subrefractive and multiple layers. Selected soundings were used in simulations to explain the effects of different types of abnormal layers on the electromagnetic propagation. Although abnormal layers did not affect ground systems, airborne ones were. For radar, a region with low or no detection is created when an abnormal layer refracts the electromagnetic energy upwards or downwards. Some combinations of multiple layers may cause effects even stronger. It is concluded that knowledge of the abnormal layers occurrence is important for operations in the Amazon region. Further, airborne radar platforms should measure local refractive conditions, if possible. A comprehensive study in time and space is recommended to provide forecasting.

THIS PAGE INTENTIONALLY LEFT BLANK

TABLE OF CONTENTS

THIS PAGE INTENTIONALLY LEFT BLANK

LIST OF FIGURES

THIS PAGE INTENTIONALLY LEFT BLANK

LIST OF TABLES

THIS PAGE INTENTIONALLY LEFT BLANK

ACKNOWLEDGMENTS

I wish to express my appreciation for those who support the completion of this thesis. I am thankful for Professor Kenneth L. Davidson for his attention, guidance and constant advise in preparing my thesis, Dr. Guest for help with AREPS, and two research members of the Meteorology Department, Mary S. Jordan and Robert Creasey, for their important help in collecting data that made possible the case study in this thesis. I am also thankful for Professor David C. Jenn for his advice and review of this work. NPS faculty members have also my gratitude for their excellent knowledge transmitted.

The Brazilian Air Force members must be thank for sending and supporting me in the NPS, in special, to those that work and worked in the Electronic Warfare Center (CGEGAR).

Finally, I would like to thank my wife Marta, and my two sons Guilherme and Nickolas, for their understanding, patience and support during our entire stay in the United States.

THIS PAGE INTENTIONALLY LEFT BLANK

EXECUTIVE SUMMARY

Systems that depend on electromagnetic propagation are affected by atmospheric conditions. Between other phenomena, significant variations in pressure, temperature, and humidity in the troposphere cause layers with abnormal refractive indexes, changing the ray paths and, consequently, the performance of those systems, both active and passive.

A system called System of Vigilance of Amazon (SIVAM) is being implemented in Brazil and uses active and passive electronic systems, ground and airborne based, to protect a vast region of forest, rivers and other natural resources. Many atmospheric phenomena occur in that region, since it is an equatorial region in South America, influenced by the Inter Tropical Convergence Zone (ITCZ) and tradewinds. Abnormal refraction layers occur frequently, indicating that the electronic systems may be affected when operated in that region.

The Global Tropospheric Experiment (GTE) conducted worldwide studies about monthly superrefraction layers and ducts occurrence, including meteorological stations in the Amazon. Three of them, Belém, Manaus and Vilhena, were examined in this thesis and showed significant seasonality. Further, a case study analyzed individual soundings from the same stations, between March and June 2003 period, allowing comparison with GTE data and simulations using the Advanced Refractive Effects Prediction System (AREPS) 2.1 software.

Simulations indicated that ground based systems were not affected by surface or elevated abnormal layers in that region, but airborne systems were by elevated layers. A sector with reduced detection (i.e., a “radar hole”) may be created when an abnormal layer refracts the radar energy downwards or upwards. The strength of this effect varies with radar and ESM parameters and layer types, especially when combined in multiple layers.

As airborne radars may be used in regions without meteorological information, a conclusion of this thesis is that the platform have some system to measure and evaluate the refractive conditions in real-time about its operational area.

This thesis is one of the first to use recent propagation modeling technology to study the occurrence of abnormal layers in the Amazon environment and its effects on the electromagnetic propagation using ultra-high frequency bands. It is recommended, however, that a more comprehensive study in time and space be done to establish a reliable forecasting about refractive conditions in the Amazon region.

I. INTRODUCTION

An expansive quantity of military systems depends on electromagnetic propagation to perform various functions, like communications, navigation, searching, tracking or fire control. Most of these systems operate in the atmospheric region between 0 and 30,000 feet. In the lower part of this region significant variations occur in temperature and humidity. These variations cause different refractive indices in the atmosphere, affecting the electromagnetic propagation and consequently the performance of those systems, both active and passive.

In Brazil, a system called System of Vigilance of Amazon (SIVAM) is being built that uses electronic systems on ground and airborne platforms to cover about 5,000,000 km^2 of forest. As the Amazon is an equatorial region in South America, many atmospheric phenomena are influenced by the Inter Tropical Convergence Zone (ITCZ) movement and the tradewinds. These phenomena lead to the formation of atmospheric layers with different refraction, which can affect the performance of radars and Electronic Support Measures (ESM) used by SIVAM.

As previous work about these meteorological phenomena and results in that region were not found, this thesis presents a first approach to study the refractive conditions in the Amazon environment and its affects on ground and airborne radar and ESM systems such as in the SIVAM system. The knowledge of abnormal refractive layers and their effects is very important, since it is necessary to operate those systems at maximum performance over that vast region.

A. PURPOSE

The purpose of this thesis is to develop a methodology of analysis for the abnormal refractive layer occurrence over the Amazon region and its effects on generic ground and airborne radar and ESM systems.

It is not intended to evaluate the performance of the SIVAM's equipment, since their parameters are classified. However, assuming generic values for the radar and ESM systems, it is possible to explain in a general sense when and how some meteorological phenomena may affect these generic systems. Different results, however, are expected when the real parameters are used. The rest of the data provided to the software simulations are from open sources, as well satellite imagery.

B. SCOPE AND METHODOLOGY

The methodology used in this thesis consists of the following analysis:

1. Abnormal Layers Occurrence and Measurements

Inserting data from a single sounding into AREPS 2.1, this software generated a graph that showed the occurrence, types, bottom and top heights of three basic types of abnormal layers, as well its combination in multiple layers.

2. Layer Occurrence and Seasonality

The layer occurrence and its characteristics were recorded using the SPSS 10.0 software for statistical processing and correlations between variables.

Occurrences during March-June 2003 were compared with past (climatologic) data, available from GTE about 1980-1985, to verify any seasonality in these occurrences.

3. Layers Selection and Comparative Effects

Surface and elevated single and multiple layers were selected to analyze their effects on radar and ESM systems. Each effect was described and related to its specific type of layer, using fixed parameters for the generic active and passive system.

C. ORGANIZATION OF STUDY

This thesis presents, in Chapter II, an overview of geographic and climatologic aspects of Amazon, as well as the SIVAM program. The next chapter, Chapter III, explores the basics of electromagnetic propagation, emphasizing the atmospheric refraction effects. Together with the reflection, they form a basis to understand the effects of abnormal layers, as well the graphics generated by simulations using AREPS.

Chapter IV presents past data about three stations in the Amazon, based on GTE computations. These data describe ducts and superrefractive layer characteristics and occurrences, using 1980 – 1985 observations. Although there are some periods without available measurements, it is possible to note some seasonality.

Chapter V makes a comprehensive analysis of abnormal layer occurrence, considering not only superrefractive layers and ducts, but subrefractive and multiple layers as well. The period analyzed was between March and June 2003, making it possible to compare results with part of the GTE data.

In addition, Chapter V presents the effects of different types of layers on the electromagnetic propagation using the AREPS software.

Chapter VI summarizes the results of the data distributions and propagation effects, establishing conclusions and recommendations for future studies.

THIS PAGE INTENTIONALLY LEFT BLANK

II. AMAZON ENVIRONMENT AND EM/SIVAM

This study of the atmosphere effects and their estimation relates to regional atmosphere properties as well as to existing or planned use of EM sensors in these areas. This section will present information on the Amazon environment relative to the geographical and climatological properties of the region (Sections A and B) and the intended EM/SIVAM system (Section C) properties.

A. GEOGRAPHICAL ASPECTS

Amazon is the region in the north of South America covered by 6.5 million square kilometers of forest, occupying large portions of the territory of nine countries: Bolivia, Colombia, Ecuador, Guyana, Peru, Venezuela, Surinam, France (French Guyana), and Brazil. About 5 million square kilometers of this jungle (approximately 76%) is located in Brazilian territory, making up almost 61% of its country's landmass.

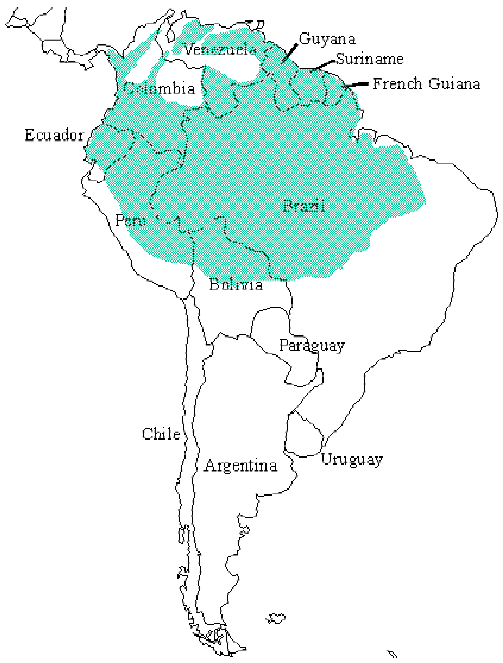

Figure 2.1 - The Amazon region (dark area in the map) covers nine countries in the South America. About 5 million square kilometers of this jungle (approximately 76% of the total) is located in Brazilian territory.

In Brazil, the Amazon Rainforest is called Legal Amazon, and embraces about 60% of the Brazilian territory, spreading over the following states: Acre, Amazonas, Pará, Rondônia, Roraima, Tocantins, west of Maranhão and north of Mato Grosso. This area is equivalent to a half of the European continent, with an area of 5,026,552 km^2, with an estimated population (in 1990) of 17,193,446 inhabitants. If compared with other countries, the size of the Brazilian Amazon is about fifty percent as large as the United States, nine times the size of France or fourteen and a half times the size of Germany. Separately, it could be the sixth largest country of the world.

Water vapor is a significant aspect of the atmosphere properties and processes. The largest basin of the world composes the hydrography of Amazon, with an area of 7,050,000 square meters, draining the lands of Brazil, Venezuela, Colombia, Ecuador, Peru and Bolivia, corresponding to 25% of South America.

The largest river of the world in flow of water, with 230,000 cubic meters of water per second, is the Amazonas River, formed by the Rio Negro River and Solimões River. Amazonas River has a declivity about 2 centimeters per kilometer, flowing in a plain that promotes slow water flow that becomes accumulated in determined points of the river. This physical condition ranks this river as the largest in the world in terms of catchments area, number of tributaries, and volume of water discharged.

The region where the Amazonian rivers run shows smaller altitudes, about 0 to 100 meters MSL (Mean Sea Level). Areas with less than 10 altitude meters are called "holms." In wet seasons, the rivers flood to these lands and deposit sediments of the plain of Amazon, allowing people to cultivate rice and jute. Lands with 10 to 100 meters of altitude are called "teso" and are not reached by water when the rivers flood.

Low Plateaus are a region in the direction of Guyana and Central Plateaus called "Firm Earth," formed by old sedimentation. Together, "holm," "teso" and "firm earth," are called the "Amazon Plain" (ThinkQuest, 2003).

B. CLIMATOLOGIC ASPECTS

High rainfall, temperatures, and humidity characterize the climate in the Amazon region during the year.

The Amazon region presents the greatest annual rainfall total in Brazil, especially notable in three main precipitation centers, located at the coast of the Amapá State, at the mouth of the Amazonas River and at the western part of the region. The first one is located in the Northwest of Amazon, with rainfall above 3000 mm/year. This center is associated with the condensation of humid air brought by easterly winds from the Intertropical Convergence Zone (ITCZ), which are high when the flow goes up to the Andes Mountains. The second center is located in the central part of Amazon, about 5º S (south of the city of Manaus), with precipitation of 2500 mm/year. The last one is located in the eastern part of the Amazonian base, near to the city of Belém, with precipitation of 2800 mm/year.

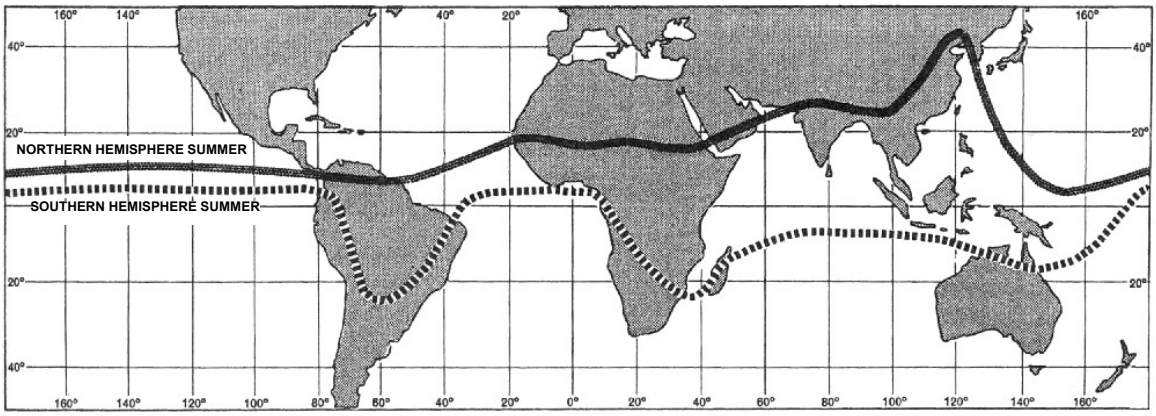

Figure 2.2 – Seasonal migration of the ITCZ in a year. During the northern hemisphere summer the ITCZ tends to be at North of the equator (continuous line) or in the South (dashed line) in the southern hemisphere summer (After: Lutgens & Tarbuck, 1982)

The North Region's rainy season (Dec-Jan-Feb) changes progressively from January-February-March, in the South of Amazon, to April-May-June, in the Northwest of the Amazonian base. This variation seems to be related to the position of the ITCZ, since the precipitation nuclei migrate from the central part of the country, in the austral

summer, to the northwest sector of South America in the austral winter, following the annual migration of the deep convection. Stations located in the Northern Hemisphere of Brazil present maximum rainfall during the austral winter (June-July-August) and minimum rainfall during the austral summer (Dec-Jan-Feb).

The rainy season in the central part of Amazon takes place in March-April-May, and in the Southern part the rainfall peak occurs in January-February-March. Rain in the Northwest of Amazon can be seen as a response to the dynamic fluctuation of the quasi-permanent convection center in this region.

The instability lines that form along the coast at the end of the afternoon cause the center of precipitation near to Belém, driven by the circulation of the sea breeze.

Other factors influence rain in the region as well, such as the penetration of frontal systems, the displacement of the Subtropical High of South Atlantic (SHSA) and the Bolivia High (Batista et al.).

Seasonal thermal amplitude is around 1-2º C while the average values are situated between 24 and 26º C. Belém presents the maximum monthly average temperature of 26.5º C in November and the minimum temperature of 25.4º C in March. In Manaus the temperature extremes are in September (27.9º C) and April (25.8º C). During winter in the Southern Hemisphere all the southern portion of the North Region, especially the southwest (Acre, Rondônia and part of Amazonas State), is frequently invaded by high-latitude anticyclones that cross the Andes Mountains in the south of Chile. Some of them are exceptionally intense, and may even cause sudden drops in temperature. Excessive daily maximum temperatures are not registered during the year, however, because the relative high moisture and intense cloudiness that characterize the region (Fisch, Marengo & Nobre, 2003).

Although it is possible to obtain much information about this vast region, much more is needed to understand and protect the Amazon. The Brazilian Government is

constructing a great technologic system, the Surveillance System of Amazon - SIVAM - that aims to do the surveillance and to get all kind of information about Amazon.

C. SIVAM

This section describes the other components considered in the assessment of effects: the sensor and radars under consideration. This is encompassed within a program, the SIVAM. The SIVAM, acronym of *Sistema de Vigilância da Amazônia* in Portuguese, that means *System of Vigilance of Amazon*, is a program that was conceived in 1990 and it is the infrastructure of a bigger system, the SIPAM, or *System for the Protection of the Amazon* (acronym of *Sistema de Proteção da Amazônia* in portuguese). SIVAM is composed of a large number of sensors and remote user stations connected to regional coordination centers by a telecommunications network.

The objective of SIVAM is to implement a surveillance and analysis infrastructure providing the Brazilian Government the necessary information for the protection and sustainable development of the Amazon region. The information generated by SIVAM is used for environmental protection, control of land occupation and usage, economical and ecological zoning, updating of maps, prevention and control of epidemics, protection of the indigenous populations, surveillance and control of the borders, monitoring of river navigation and forest fires, identification and combat against illegal activities and air traffic control and surveillance for cooperative and non-cooperative aircrafts. To do these, it is necessary the use of modern sensing technologies.

The SIVAM has three Regional Surveillance Centers in Manaus, Porto Velho, and Belém, as well as at the General Coordination Center in Brasilia. Networks of computer workstations provide processing of satellite images, the development and use of application software and program development tools, the management and use of extensive databases from the most varied sources, as well as for the training and specialization of system users (Raytheon, 2002).

On July 25, 2002 the President Fernando Henrique Cardoso inaugurated the SIVAM that is installed, with important participation of the Brazilian industry and technicians, and will be operated exclusively by Brazilians, thus conserving the strategic destination of Brazilian resources in Brazilian hands.

1. SIVAM Assets

The SIVAM uses modern up-to-date equipment to achieve its goals. There are many different components and the most important are listed below (Aviation Today, 2002).

SENSORS

- 7 ASR-23ss Primary/Monopulse Secondary Radars
- 7 Condor Mk 2 Secondary Radars
- 6 Transportable TPS-B34 Primary/Secondary Radars
- 5 Embraer EMB 145-based Surveillance Aircraft
- 3 Embraer EMB 145-based Remote Sensing Aircraft
- 10 Weather Radars
- 295 Sensors: Weather (81), Lightning (14) and Hydrologic (200)
- 5 Satellite Imagery Receivers
- 4 Instrument Landing Systems
- 3 HF Direction Finding Systems

TELECOMMUNICATIONS

- 424 Very Small Aperture Satellite Ground Terminals
- 26 Satellite Trunking Terminals
- 5 SATCOM Hub Stations
- 32 Ground-to-Air Radio Stations (224 Radios)
- 21 Remote Telecommunications Switching Stations
- 1,028 Data Access Terminals

DATA PROCESSING

- 1 En-Route ATC Center
- 3 Regional Coordination Centers
- 1 General Coordination Center

TEST AND CERTIFICATION

- 4 Hawker 800XP-based Flight Inspection Aircraft

Although there are many types of equipment for a great variety of purposes in the SIVAM, this thesis will focus only on the primary radars (ground and airborne-based), and on the equipment to intercept and locate electromagnetic signals in radar bands. It is justified by the fact that it is more important for the Electronic Warfare issues to detect actively or passively non-cooperative targets. Secondary radars work with the response of auxiliary equipments in cooperative targets, like an IFF or transponder.

As the parameters of SIVAM radars and ESM systems are classified, but they are needed for simulations in this thesis, generic values will be assumed. Although the results of these simulations will differ from those when using real systems values, they will be sufficient to explain the effects of refractive conditions in the Amazon.

D. SUMMARY

About 5 million square kilometers of Amazon jungle are located in Brazilian territory. High rainfall occurrence, temperatures, and humidity characterize its climate during the year. For protection and development of this region, the Brazilian Government is implementing surveillance and analysis infrastructure, called SIVAM, composed of a large quantity of sensors and remote user stations connected to regional coordination centers by a telecommunications network.

THIS PAGE INTENTIONALLY LEFT BLANK

III. ELECTROMAGNETIC PROPAGATION

A. ATMOSPHERIC REGIONS

Electromagnetic waves traveling in the earth's atmosphere are affected by many factors varying with height, geographical location and even in time (period of the day and seasonality). Three main regions, troposphere, stratosphere and ionosphere, divide the earth's atmosphere, each one, with its particular importance to the electromagnetic propagation.

As shown in Figure 3.1, the ionosphere extends upward from about 50 km up to 400 km. It is formed by free electron layers and enables long distance links using refracted "sky waves" for frequencies between, approximately, 3 MHz and 30 MHz. Some radar systems, called Over the Horizon Radar (OTHR), use this effect to provide very long-range detection. These systems, however, are not used by the SIVAM program.

The stratosphere is located between the troposphere and ionosphere. In this region, there are no free electron maxima, there is little water vapor, and its temperature is almost constant, having no significant effects on electromagnetic propagation.

The troposphere extends from the surface up to about 6 km at the poles, and 18 km at the equator. In this region almost all types of weather conditions take place, like formation of clouds and fronts, rain, and variations of temperature, pressure and humidity. This region and the earth's surface have the main effects on the propagation of the electromagnetic waves.

Considering a transmitter located in the troposphere, the electromagnetic waves have three different ways to reach a receiver or a target. One is using ground waves, radio waves that travel near the surface using vertical polarization. Another way is by sky waves, or waves that are reflected by the ionosphere back to the earth. The last is using the space waves that normally follow two distinct paths, direct or reflected by the ground or another obstacle. (NAVEDTRA, 1983, pp. 2-11 – 2-15)

Although electromagnetic waves may propagate by different mechanisms, this thesis will consider only the propagation by space waves (direct and reflected). The frequency band used in radar systems is normally between 200 MHz and 40 GHz, and sky or ground waves are important only for lower frequencies, below 40 MHz.

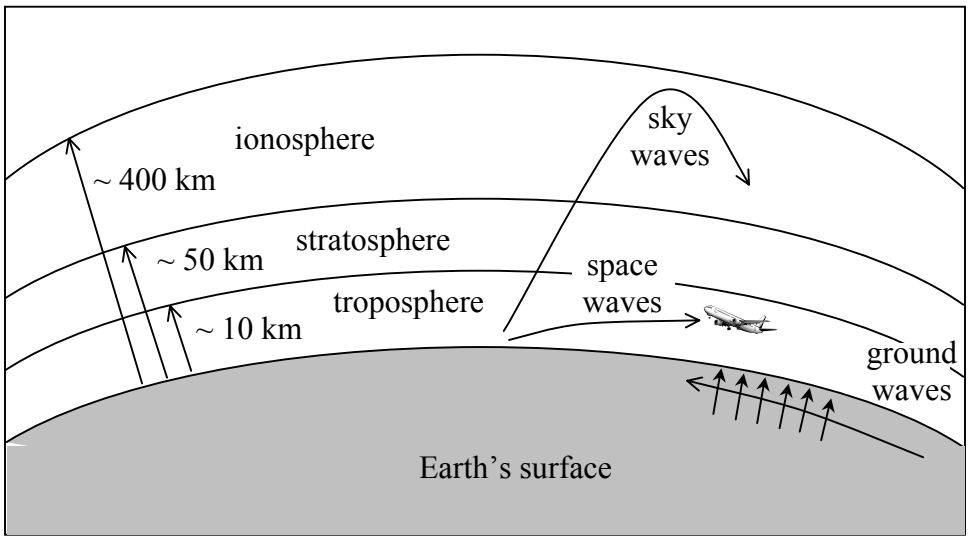

Figure 3.1 – The main atmospheric regions and modes of propagation.

The earth's surface is the main cause of reflection. When a radar transmits to a target, its energy follows the direct and reflected paths. The radar return echo follows the same two paths, as shown by the Figure 3.2.

The magnitude of the resultant target echo back in the radar antenna depends on the amplitude and relative phases of this signal. These two factors depend on many others, like range between target and radar, antenna and target heights, frequency, polarization, and surface reflection coefficient. As a result, the radar coverage is not formed by a uniform volume of space, but by a lobed elevation pattern. If an aircraft is flying at a constant altitude, for a fixed ground radar, its tracking will not be continuous, as illustrated by the Figure 3.3.

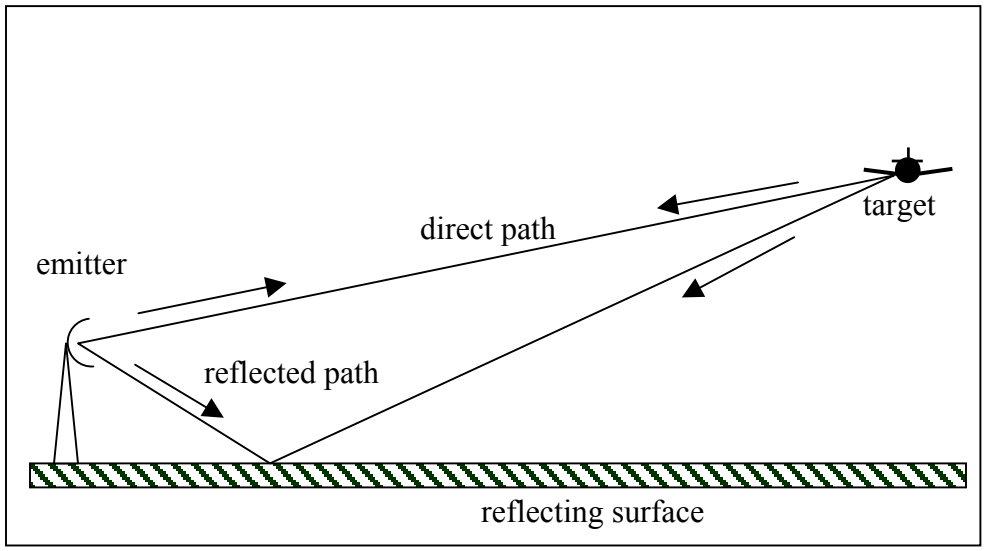

Figure 3.2 – Illustration of the direct and reflected paths between a radar and a target.

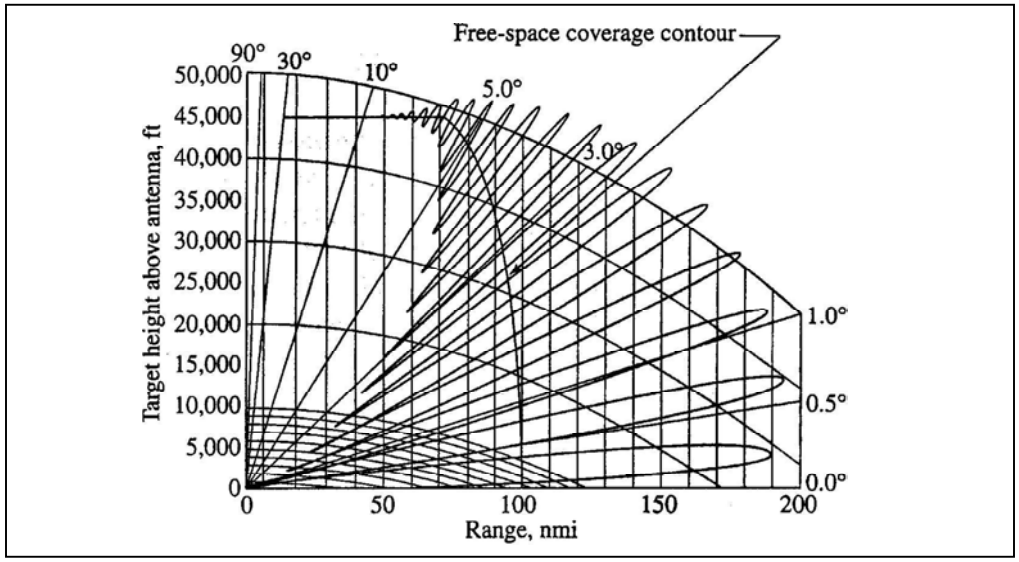

Figure 3.3 – Reflections in the Earth's surface cause a radar coverage composed by many lobes, different from the free-space situation (From: Skolnik, 2001, p. 491)

Another important effect is caused by the refraction, or bending of the waves' path. As the atmosphere varies in temperature, humidity, pressure, and density with height, it causes a variation in velocity of propagation, and the waves tend to bend in the direction of the slowest medium.

Normally the effect of the atmospheric refraction is favorable, increasing the radio and radar horizon beyond the geometric horizon. However, the atmosphere characteristics are not constant and the refraction may vary significantly with the height. To understand and measure the refraction variation in some particular area, it is useful to build a refractivity profile, i.e. a graph showing the index of refraction with the height. Two basic instruments, a radiosonde or a microwave refractometer, are used with this purpose.

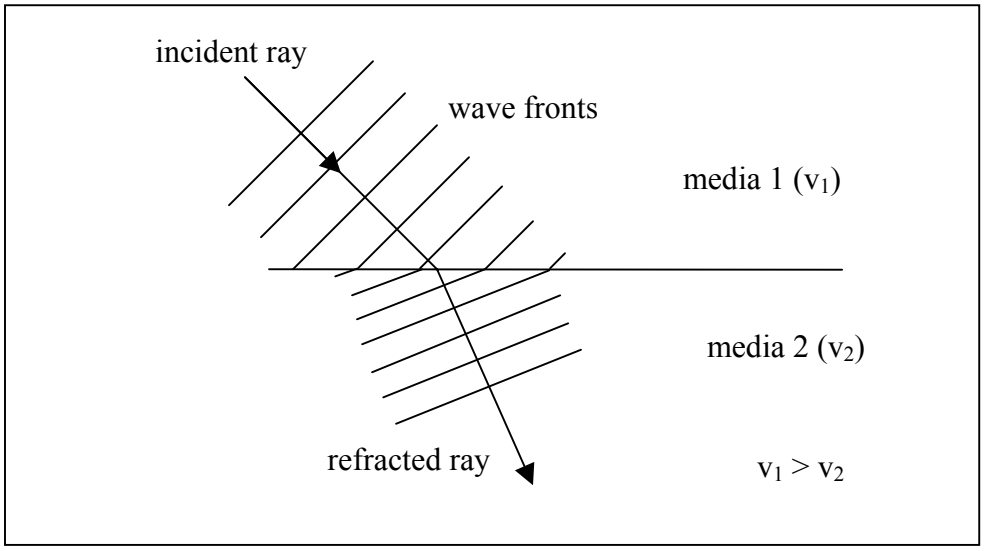

Figure 3.4 – The difference of velocity of propagation between two medias causes a changing in the rays paths, bending to the slowest media. This effect is called refraction.

A radiosonde indirectly measures the refractivity profile, using the empirical relationship between water vapor pressure (humidity), temperature and atmospheric pressure. The most common way is using a balloon, routinely launched throughout the world twice a day, at 00:00 and 12:00 GMT. The balloon carries the instruments up to more than 30,000 feet and transmits its data to the ground station. The measurements, however, are valid for a limited time, since the atmospheric conditions are dynamic. The spatial area covered may be small. Similar equipment may be used in helicopters or rockets.

Another way of measuring refractivity is using the refractometer. This instrument directly measures the index of refraction by comparing the resonant frequencies of two

identical microwave cavities. This instrument has much greater accuracy than the indirect measurements, about 0.1N unit. This instrument, however, is usually too costly to be expendable, as for a radiosonde or a rocketsonde normally carried by aircraft.

Aircraft may be used to obtain meteorological information about areas without sounding services. If using a refractometer, a vertical profile should be built, but it is limited by the aircraft height variation. One alternative is for sensors, like those used in balloons, were released by gravity from the aircraft, transmitting its signals back to it. In this case, however, the vertical profile should cover only heights below the aircraft.

B. ATMOSPHERIC REFRACTION

The refraction in the atmosphere is due the variation of the velocity of propagation with height. The ratio between the velocities of the propagation in a vacuum and the atmosphere gives the index of refraction n of the atmosphere. The difference between these two velocities is small, for example, a typical index of refraction at mid-latitudes is about 1.000315 (Skolnik, 2001, p. 495). For convenience, is preferable the use of the modified index of refraction, N, called refractivity and defined by $N = (n\text{-}1)10^6$. The refractivity N for frequencies between 100 MHz and 80 GHz in the atmosphere is given by the equation (Davidson, 2003, p. 3-7)

$$N = (n-1).10^6 = 77.6\frac{P}{T} - 5.6\frac{e}{T} + 3.75\left(10^5\frac{e}{T^2}\right) \qquad (1)$$

where:

P = barometric pressure in millibar

e = partial pressure of water vapor in millibar

T = absolute temperature in K degrees

The barometric pressure and water vapor content decreases more rapidly than the absolute temperature with the height, so, the refractivity N tends to decrease with height. Normally it causes a bending downward of the propagation, increasing the radio and

radar horizon. Among the gasses present in the atmosphere, water vapor is the most important to the refraction, since it is the only gas with dipole moment.

The major changes in atmospheric refractivity occur in the vertical dimension, but its absolute value at some particular altitude is not so important as the gradient of refractivity. The gradient of refractivity causes the rays to bent downward and it is really significant in the vertical direction.

Geometrically, the height z above the earth's surface with the radius r_e, following a tangent straight line in the distance d is approximated by the expression $z = d^2/2r_e$. However, the refraction causes a bending of the rays, and the radius of the ray's curvature can be determined by $r=10^6/(dN/dz)$. In this case, the expression to determine z becomes (Op. Cit., p 3-13)

$$z = z_1 - z_2 = \frac{d^2}{2}\left(\frac{1}{r_e} + \frac{10^6}{(dN/dz)}\right) \qquad (2)$$

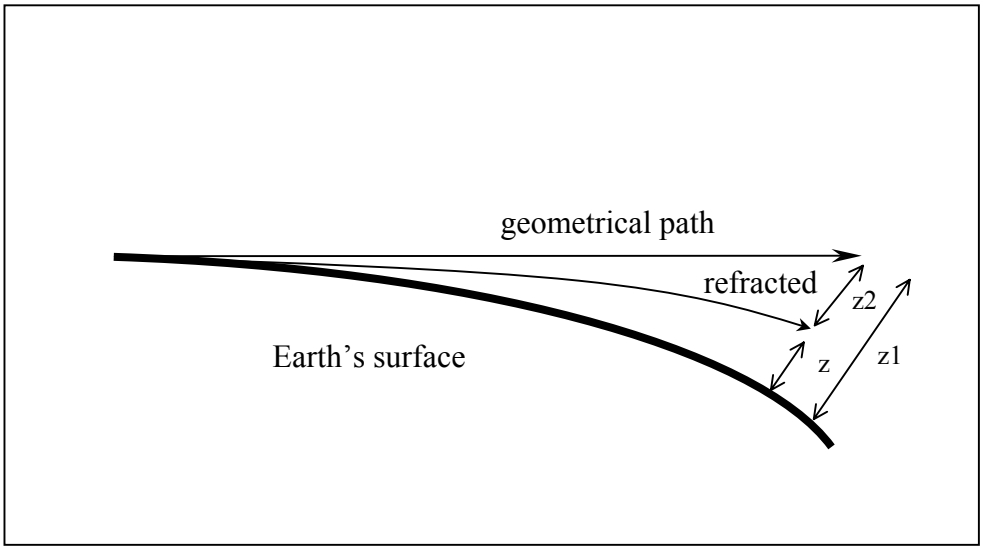

Figure 3.5 – The horizon to the electromagnetic waves is normally bigger than to the geometrical view (After: Davidson, 2003, p. 3-13).

For standard conditions (-40 N/km), the refraction causes a curved path with radius r = 25,000 nmi, approximately 4 times the earth radius. Using this fact in the last equation, it becomes

$$z = z_1 - z_2 = \frac{d^2}{2}\left(\frac{1}{r_e} - \frac{1}{4r_e}\right) = \frac{d^2}{2}\left(\frac{3}{4r_e}\right) \qquad (3)$$

It is almost the same of the original $z=d^2/2r_e$, but using an earth radius multiplied by 4/3. The earth's radius of 4/3 is important because most of graphical representations use it, i.e. AREPS, and the radio and radar horizon is 33% larger than the geometrical horizon. Graphically, the earth's radius is increased by 4/3, less curved, and the rays are straight for standard conditions.

Numerically, the radio horizon can be estimated by the following equation (Skolnik, 2001, p. 496):

$$d_{nmi} = 1.23\sqrt{h_{ft}} \qquad (4)$$

where:

d_{nmi} = distance between the emitter and the horizon in nautical miles

h_{ft} = antenna height in feet.

This equation, however, presents only an initial idea of the distance, since N may vary significantly. In fact, a normal refraction is considered when the refractive gradient with height, dN/dh, is between 0 and -79 N/km. Gradients between -79 and -157 N/km indicate superrefraction, and the rays tend to bend more over the earth's curvature than in the normal refraction case. On the contrary, if the gradient increases with height, instead of decreasing, the rays may curve upward, reducing the horizon, which is called subrefraction. When the gradients exceed -157 N/km, the curvature of the propagating rays exceeds the curvature of the earth and this trapping layer forms a duct. The ducted energy may travel for distances far beyond the standard horizon, as shown in Figure 3.6.

A modified index of refractivity M, however, is more useful than N to represent refractive conditions, especially for occurrence of ducts. This modified index is defined by

$$M = N_z + 157_z \qquad (5)$$

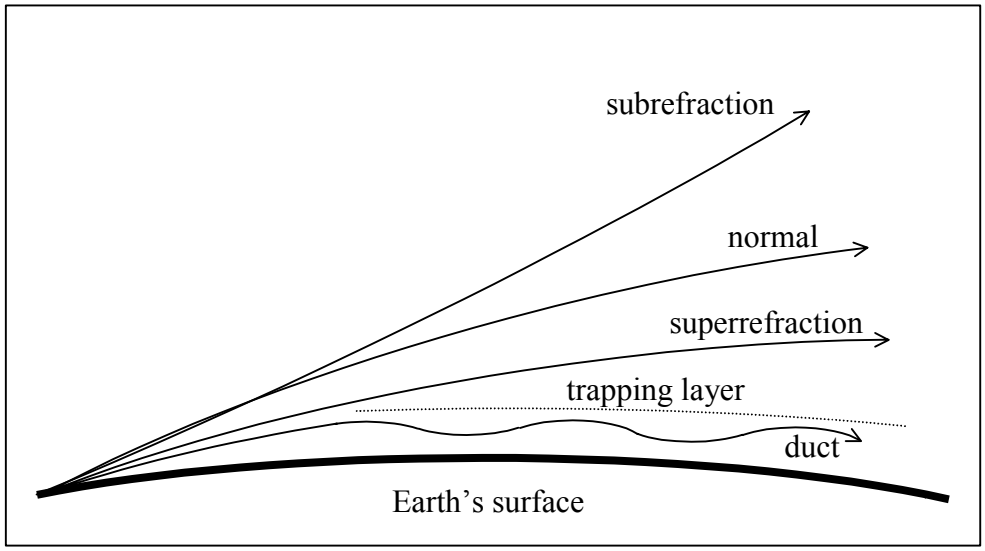

Figure 3.6 – Atmospheric refraction cause subrefraction, superrefraction, normal refraction or trapping layers that form ducts (After: Davidson, 2003, p. 3-18).

When M = 0, the rays have the same earth's curvature (superior limit of superrefraction). The presence of ducts, therefore, is showed by a negative M. Graphically, the M and N profiles may be compared as shown in the example on the Figure 3.7. Table 3.1 summarizes a comparison between N and M. These conditions have important effects on the radar propagation, as discussed in next section.

Refractive condition	N units / km	M units / km	Radio horizon
Subrefraction	More than 0	More than 157	Reduced
Normal	Between 0 and –79	Between 157 and 78	Standard
Superrefraction	Between –79 and –157	Between 78 and 0	Increased
Trapping	Less than –157	Less than 0	Increased

Table 3.1 – Comparison between N and M units

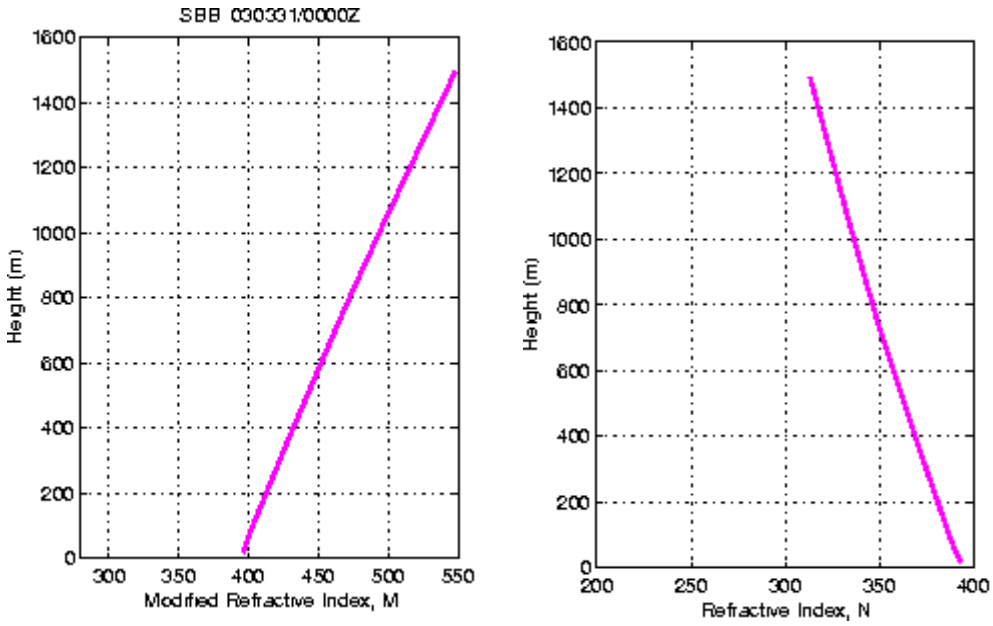

Figure 3.7 – Example of one *M* profile and a *N* profile of the same station and same time. The difference is basically the relative inclination of the slope. These graphs were generated by MATLAB code using a real sounding data.

C. EFFECTS OF ATMOSPHERIC REFRACTION ON RADARS

If the refractive conditions in some region present a modified gradient of refractivity *M* between 157 and 78 M/km (or between 0 and -79 N/km), is considered normal, or standard refraction. With standard refraction, the radar horizon may be estimated by the equation (Skolnik, 2001, pp. 496, 519):

$$D_{nmi} = 1.23(\sqrt{h_{antenna}} + \sqrt{h_{target}}) \qquad (6)$$

where:

D_{nmi} = distance between the radar antenna and the target in nautical miles

$h_{antenna}$ = radar antenna height in feet

h_{target} = target height in feet.

For a ground-based radar, searching for low altitude targets, this condition is favorable in that it increases the geometric horizon about 33% (4/3 of the earth's radius).

On the other hand, the downward bending caused by normal refraction causes an error in determining the target altitude for height-finder radars.

For refractive conditions when *dM/dh* is outside 157 and 78 /km are called anomalous, abnormal, or nonstandard conditions. They are the cases of subrefraction and superrefraction or ducts.

When the *dM/dh* is above 157 /km (equivalent to a *dN/dh* positive), subrefraction, or substandard propagation, occurs. The rays tend to bend upward, decreasing the radar horizon. Although a rare condition, its effect can be serious. It has been suspected of causing ship accidents when using marine radars (Skolnik, 2001, p. 502). Subrefraction occurs normally when warm air flows over a cool surface or cooler air mass.

In another situation, if *dM/dh* is between 89 and 0 M/km, the radar horizon increases with the ray's tendency to bend downward, following the earth's curvature. A gradient, *dM/dh*, equal to 0 /km means that the effective earth's radius becomes infinite (no curvature). In this case, the rays and the earth's surface will be parallel.

When the *dM/dh* gradient is less than 0 (a negative *M* gradient), the rays nearly parallel to this trapping layer exceed the earth's curvature and they are send back to the surface, forming a duct. There is a difference, therefore, between trapping layers and ducts. Trapping layer is the region where *dM/dh* is negative and the rays bend strongly downward. Below this region, the rays tend to bend (relatively) upward. The combination of these downward and upward paths forms a duct.

A duct is the region associated with a trapping layer where the electromagnetic waves are confined and channeled. A duct is a waveguide for which the top is always a trapping layer, but the bottom may be the reflecting surface (*surface based duct*) or above the surface (*elevated duct*). They are depicted in Figure 3.8.

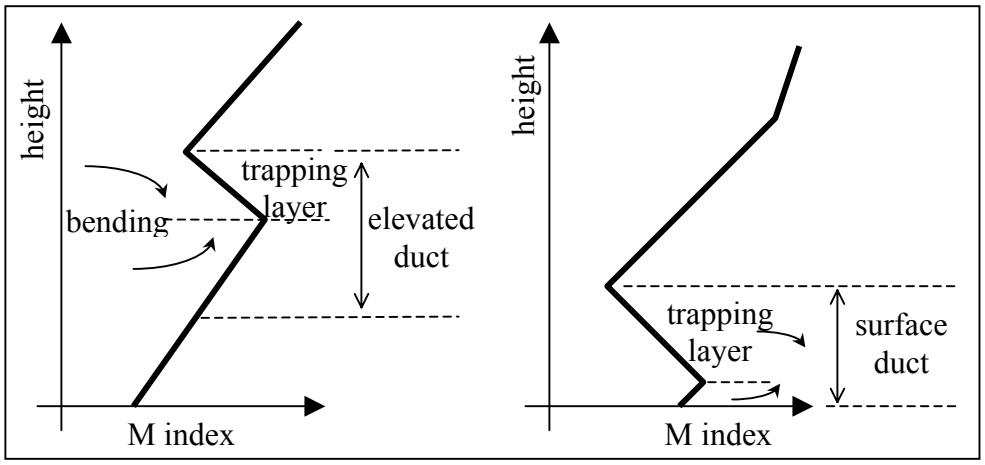

Figure 3.8 – *M* profile showing an elevated duct formation, as well one surface duct. (After: Davidson, 2003, p. 3-23).

In addition, to propagate energy within the duct, the angle of incidence and the minimum frequency are significant factors. The angle must be small, usually less than one-half degree; therefore, only the incident rays nearly parallel to the duct are trapped. The frequency is related to the thickness of the duct. In a general sense, higher frequencies (smaller wavelengths) tend to be ducted more easily than lower frequencies (bigger wavelengths). Although there is no a well-defined frequency cut-off for a determined duct thickness, an empirical relation is approximated by (Op. Cit., p. 3-32):

$$f_{\min} = 3.6 \times 10^{11} \times d^{-3/2} \qquad (7)$$

where:

f_{min} = minimum trapped frequency in Hz

d = duct thickness in meters

The Table 3.2 shows some minimum estimated frequencies versus duct thickness.

f_{min} (MHz)	Wavelength (m)	Duct thickness (m)
150	2.00	179.0
192	1.56	152.0
220	1.36	138.0
425	.706	89.6
1000	.300	50.6
3000	.100	24.3
5800	.052	15.6
8500	.035	12.2
9600	.031	11.2
10250	.029	10.7
15000	.020	8.30
30000	.010	5.24

Table 3.2 – Examples of minimum trapped frequencies versus duct thickness.

Ducts are formed in three general cases: (1) evaporation ducts that occur normally at the surface of the sea, (2) surface-based and (3) elevated ducts that occur over land as well over water. In this thesis, however, the evaporation duct will not be analyzed, since the region of study is above land.

D. ELECTROMAGNETIC PROPAGATION SUMMARY

The atmosphere is not a homogeneous medium, especially in the troposphere. In its lower part, the Earth's surface reflects electromagnetic waves forming lobes that affect the radar coverage. From the surface up to, approximately, 30000 feet high, the troposphere has significant variations of temperature, humidity and pressure with height, forming layers with varying refractive index.

Under normal refraction conditions, electromagnetic waves in the VHF and UHF bands are slightly bent downwards, having a radio or radar horizon farther than the geometric horizon. If the refractive index decreases with height more than the normal, as in a superrefractive layer, the waves bend more downwards, following the Earth's

curvature and increasing the radar horizon at low altitudes. If the refractive index decrease exceeds a Earth radius defined limit, $dM/dh < -157$ /km, the electromagnetic waves are trapped in a layer that forms a duct. The minimum frequency trapped is inversely proportional to the duct thickness.

If the refractive index decrease with height (dM/dh), on the other hand, is less than the normal, as in a subrefractive layer, the waves have less downward bending, or may even bend upwards, decreasing the radar horizon for low altitudes.

THIS PAGE INTENTIONALLY LEFT BLANK

IV. REFRACTIVE CONDITIONS OF THE AMAZON ENVIRONMENT

The region between the semi permanent high-pressure areas at 30º North and 30º South and the equator is called the tradewinds. The Amazon is located in the Southern part of this region. The tradewinds offer favorable conditions for the occurrence of ducts, since this higher air flux between the high-pressure areas and the equator may have significant differences from the atmosphere below.

Large-scale subsidence occurs in the high-pressure region. It is a slow sinking of dry air over the low-level marine air, flowing toward the equator. In the underlying boundary layer, the air is relatively cool and moist compared to the overlying air. Above the boundary layer, the warm and dry subsiding air causes the tradewind inversion, where gradients lead to the formation of elevated trapping layers and ducts. Lower duct formations may be found as well, at the cloud-base level (about 2000 feet) and over the water.

D. L. Ringwalt and F. C. MacDonald (1961, pp. 377-383) conducted a field experiment on elevated duct propagation in the tradewinds in November and March 1959, using two aircraft carrying radio transceivers at 200 MHz. They flew between Recife (northeast of Brazil) and Ascencion Island, separated about 1200 nautical miles. Link distances between 500 and 1250 nmi was found in 14 flights made in November, the seasonal optimum for ducting formation. In March, when it approaches the season of minimum ducting occurrence, the distances were about 150 nmi less.

The Global Tropospheric Experiment (GTE) in 1985 published comprehensive data about the occurrence of tropospheric ducts and superrefractive layers (SRLRs) in many parts of the world, as well in the Amazon region, using five years of observations (Ortenburger, Lawson & Patterson, 1985). These data were used in this thesis in a first analysis about the occurrence of abnormal layers in Belém, Manaus and Vilhena, shown in the map of the Figure 4.1. The location of these three stations is given in the Table 4.1.

Station	Latitude	Longitude	Elevation MSL (ft)
Belém	01º 22’ S	48º 28’ W	48
Manaus	03º 09’ S	59º 58’ W	252
Vilhena	12º 43’ S	60º 07’ W	1956

Table 4.1 – Coordinates and height (MSL) of Belém, Manaus and Vilhena stations.

Figure 4.1 – Location of the three stations studied.

Vilhena is the one with less available data, especially in April (only two soundings accepted) and May (no sounding was accepted), as shown in the Table 4.1.

Station	Jan	Feb	Mar	Apr	May	Jun	Jul	Aug	Sep	Oct	Nov	Dec	Total
Belém	34	39	35	45	30	14	22	21	30	21	20	30	341
Manaus	42	37	35	35	22	37	40	28	52	32	22	37	419
Vilhena	19	14	10	2	0	14	18	18	13	12	9	5	134

Table 4.2 – Number of soundings computed by Ortenburger, Lawson & Patterson (GTE data).

A. SURFACE DUCT OCCURRENCE

The Figure 4.2 shows the percentage of surface duct occurrence at the three stations. Surface ducts in Manaus and Vilhena show some seasonality, as show in the Figure 4.3. Manaus shows lower values only in October and November.

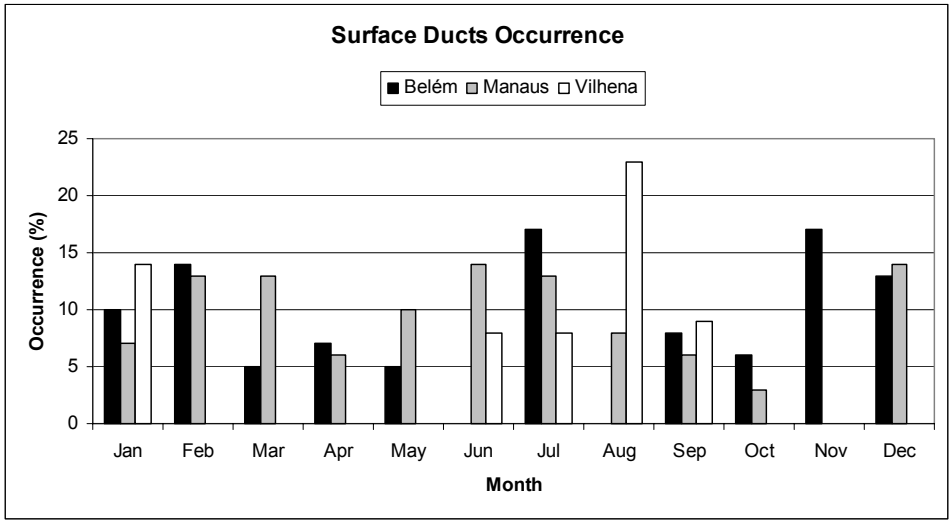

Figure 4.2 – Percentage of surface duct occurrence in Belém, Manaus e Vilhena (Ortenburger, Lawson & Patterson, 1985).

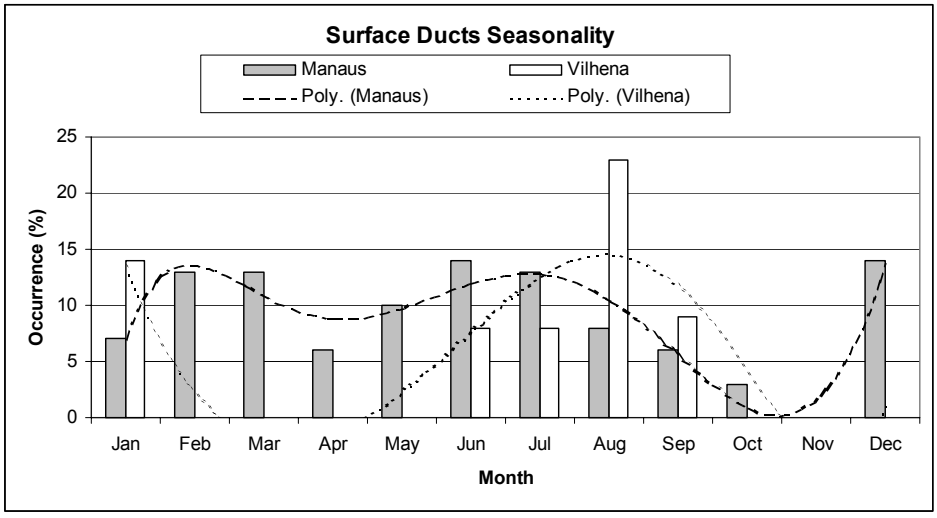

Figure 4.3 – Surface ducts show some seasonality, especially Manaus and Vilhena. Belém did not show a predictable occurrence (Ortenburger, Lawson & Patterson, 1985).

Figure 4.4 presents the median value of the height of surface ducts by month. The surface duct height is important because it is used to estimate the minimum trapped frequency. Table 4.3 shows the annual median heights and the corresponding minimum trapped frequency.

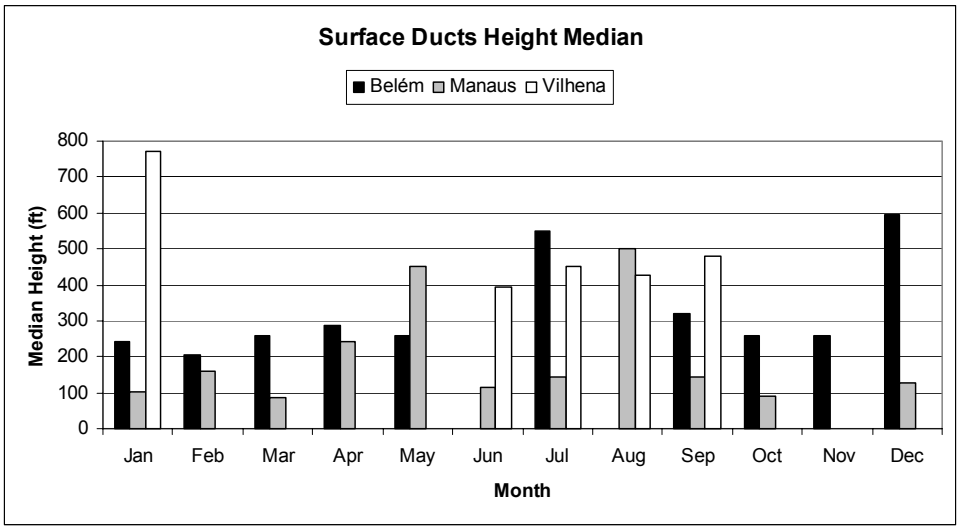

Figure 4.4 – Median height of surface ducts of Belém, Manaus and Vilhena stations (Ortenburger, Lawson & Patterson).

Station	Annual surface duct median height (ft)	Minimum trapped frequency (MHz)
Belém	237	452
Manaus	105	1650
Vilhena	426	464

Table 4.3 – Annual surface duct median height and the correspondent minimum trapped frequency (Source: Ortenburger, Lawson & Patterson, 1985).

Many long-range ground radars use frequencies from about 1500 MHz and below. It means that the duct heights in the three stations tend to trap waves from this type of system, especially Belém and Vilhena.

B. SURFACE SRLR OCCURRENCE

The Figure 4.5 shows the percentage of surface SRLR occurrence at the three stations. Although a weaker effect on electromagnetic propagation than ducts, superrefraction layers still tend to increase the radar and ESM detection, refracting the rays downwards, increasing the horizon. Figure 4.6 shows the seasonality of the surface SRLR in Vilhena. The other stations did not show predictable behavior.

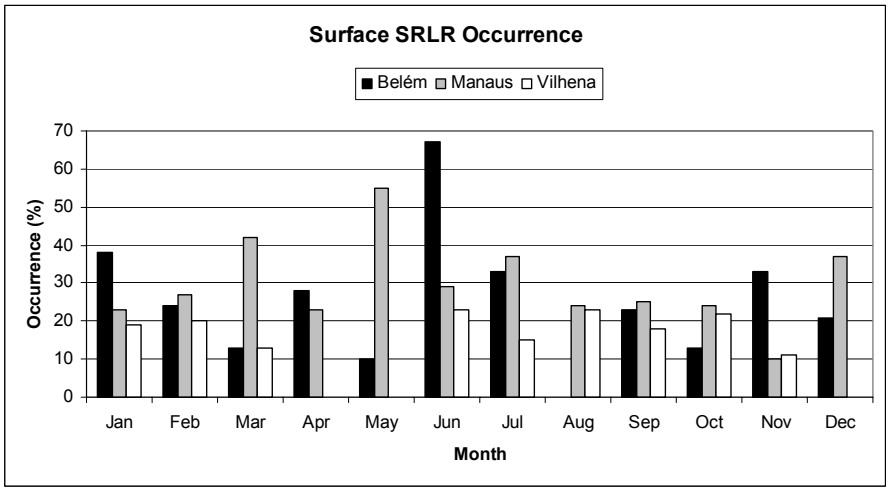

Figure 4.5 – Percentage of surface SRLR occurrence in Belém, Manaus and Vilhena (Ortenburger, Lawson & Patterson, 1985).

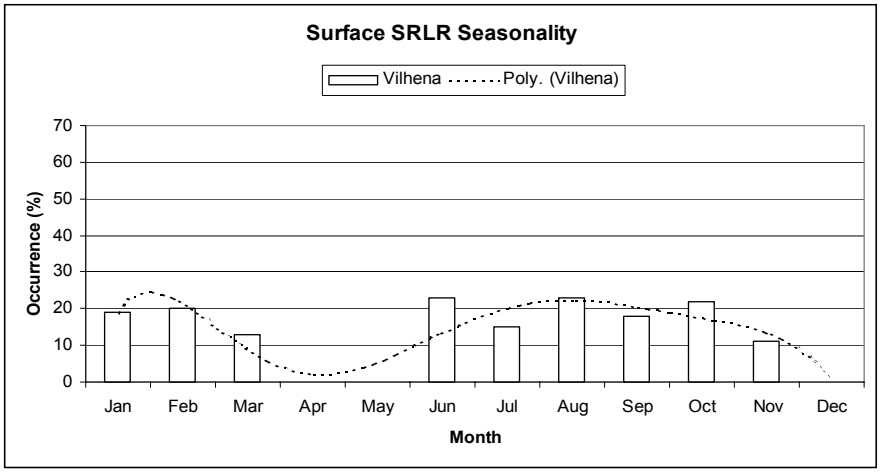

Figure 4.6 – Trendline about the surface SRLR occurrence in Vilhena (Ortenburger, Lawson & Patterson, 1985).

C. ELEVATED DUCT OCCURRENCE

The Figure 4.7 shows the occurrence of elevated ducts at the three stations during the year. The station with the highest occurrence is Belém.

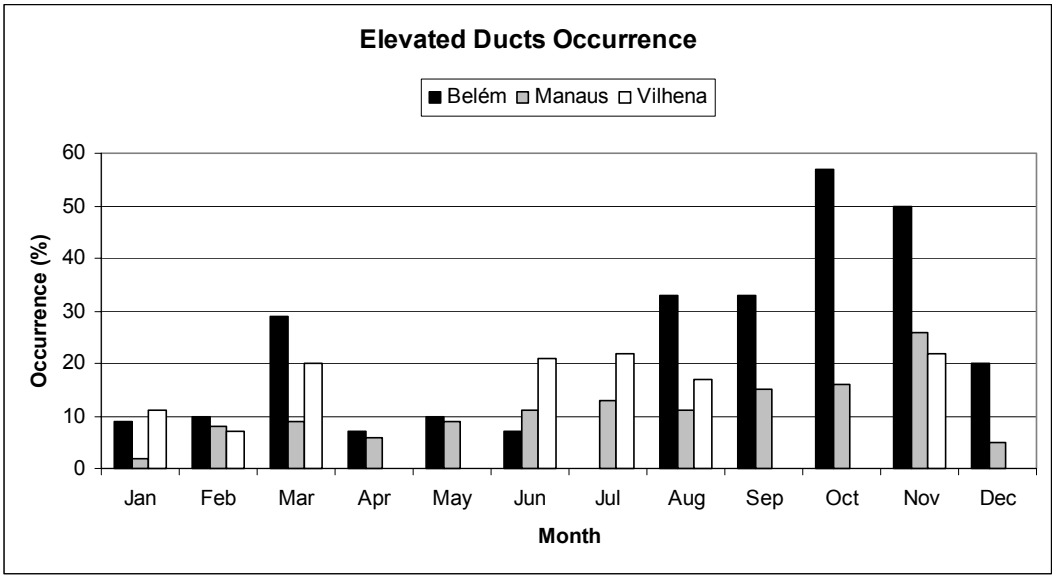

Figure 4.7 – Percentage of elevated ducts occurrence (Ortenburger, Lawson & Patterson, 1985).

Based on the GTE data, the occurrence of elevated ducts in Belém and Manaus shows some seasonality, as evidenced by the trendlines in the Figure 4.8. The maximum occurrence is between August and December. This period coincides with the "dry" season in the Amazon, as well with the transit of the ITCZ from North to South hemisphere. Data from Vilhena station did not show a periodic occurrence.

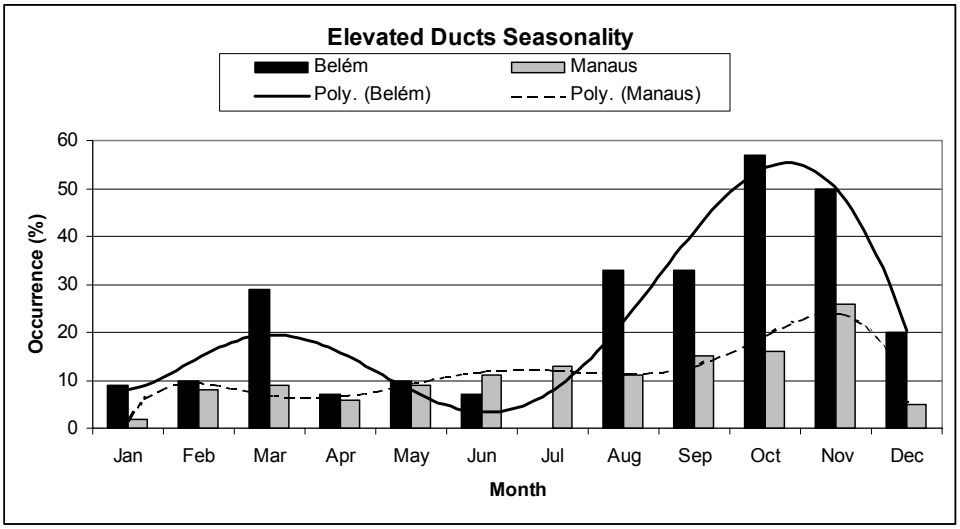

Figure 4.8 – Trendlines of elevated ducts occurrence in Belém and Manaus. (Ortenburger, Lawson & Patterson, 1985).

The elevated duct height top median show great variability during the year, as shown in the Figure 4.9. The annual elevated duct median thickness is shown in Table 4.4, as well the corresponding minimum trapped frequency.

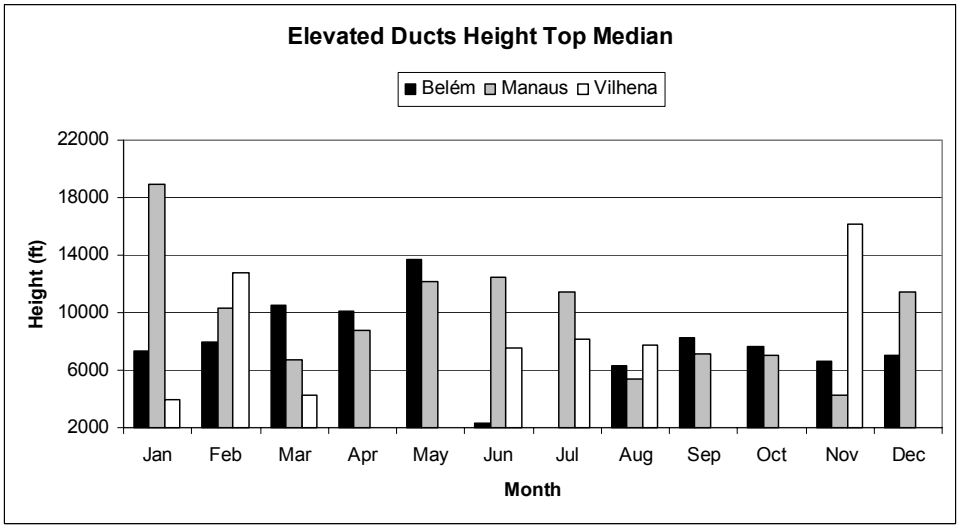

Figure 4.9 – Duct height top median of elevated ducts in Belém, Manaus and Vilhena (Ortenburger, Lawson & Patterson).

Station	Annual elevated duct median thickness (ft)	Minimum trapped frequency (MHz)
Belém	381	383
Manaus	291	712
Vilhena	113	339

Table 4.4 – Annual elevated duct median height and respective minimum trapped frequency (Ortenburger, Lawson & Patterson, 1985).

The elevated ducts tend to trap frequencies below 1500 MHz, especially Belém e Vilhena, below 450 MHz, the band for long-range radars.

D. ELEVATED SRLR OCCURRENCE

The Figure 4.10 shows the occurrence of the elevated SRLRs at the three stations.

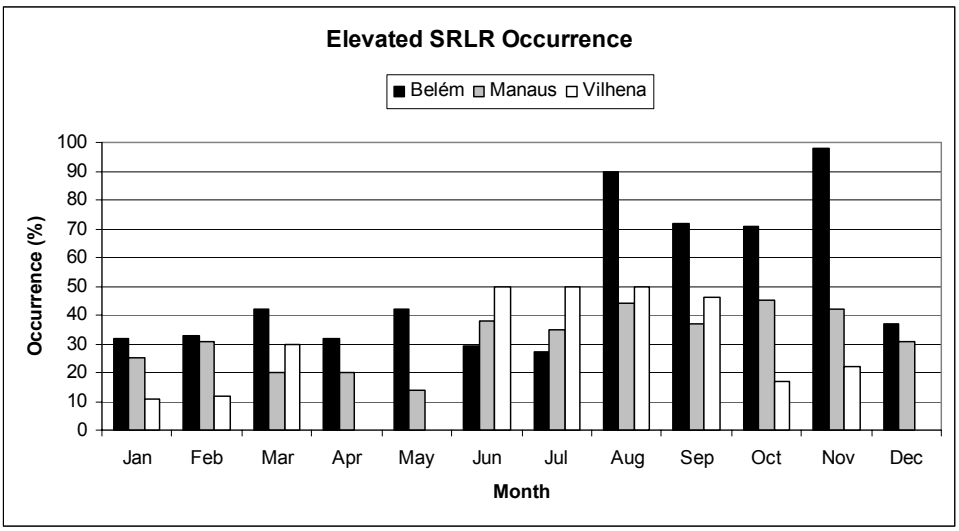

Figure 4.10 – Occurrence of elevated SRLRs in Belém, Manaus and Vilhena (Ortenburger, Lawson & Patterson, 1985).

Elevated SRLR have more occurrences between August and December for Belém and Manaus, and between June and September for Vilhena, as shown by the Figure 4.11.

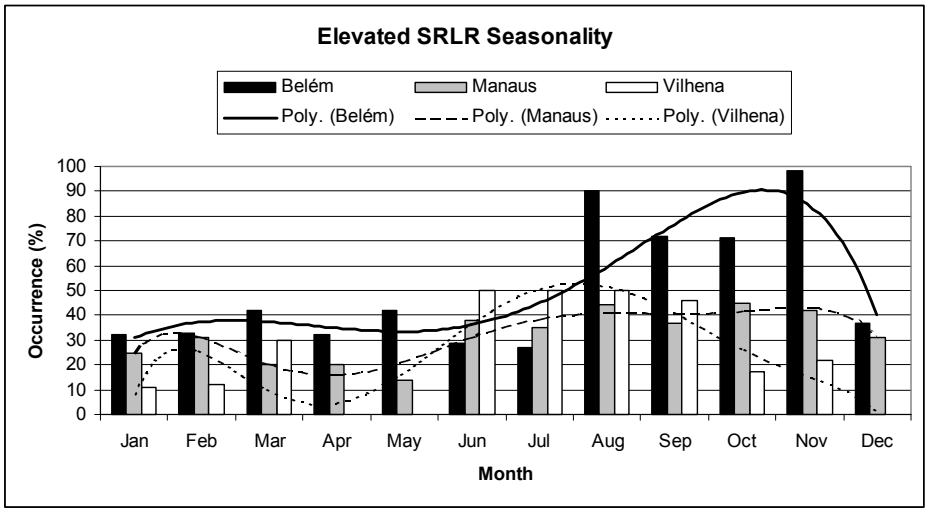

Figure 4.11 – Seasonality of elevated SRLR over the three stations analyzed (Ortenburger, Lawson & Patterson, 1985)

E. DIURNAL VARIATIONS IN THE LAYERS OVER THE AMAZON

Observations during the Amazon Boundary Layer Experiment (ABLE 2A, wet season) indicate that the mixing layer over the Manaus region grows rapidly at 5-8 cm/sec soon after sunrise as the surface sensible heat flux becomes positive. Maximum rates up to 10 cm/sec can be found within 2 hours after the sunrise. Under undisturbed conditions (no rainfall and smooth variations in temperature and solar radiation), no horizontal discontinuities were noted in the mixed layer depth over distances of 300-400 km. Its height reached 3000 ft by 11:00 LT and remains above this up to 16:00 LT. At 13:00 LT the mean maximum height of 3600 ft was reached (Martin et all., 1988, p. 1361-1375).

Worldwide, the soundings occur normally twice a day, at 00Z and 12Z. Since the three stations are located in the UTC-4 zone, most of the data is relative to 08:00 local time (LT), as shown in Table 4.4. At these stations, the sunrise and the sunset is about 06:00 LT and 18:00 LT respectively, without significant differences during the year.

This means that, since many abnormal layers may occur between the ground and 3600 ft, important variations during the day and its possible impact on abnormal layer

occurrence will not be considered. Table 4.5 shows the number of soundings by month and time of the three stations. Most of the soundings occurred at 12:00Z.

Station	Time	Jan	Feb	Mar	Apr	May	Jun	Jul	Aug	Sep	Oct	Nov	Dec	Total
Belém	00Z	0	0	0	0	0	0	1	0	7	0	0	0	8
UTC-4	12Z	34	39	35	45	30	14	21	21	23	21	20	30	333
Manaus	00Z	0	0	3	1	0	8	11	5	16	0	0	0	44
UTC-4	12Z	42	37	32	34	22	29	29	23	36	32	22	37	375
Vilhena	00Z	0	0	0	0	0	0	0	0	0	0	0	0	0
UTC-4	12Z	19	14	10	2	0	14	18	18	13	12	9	5	134

Table 4.5 - Number of accepted soundings by month and time about Belem, Manaus and Vilhena stations (Ortenburger, Lawson & Patterson, 1985).

F. REFRACTIVE CONDITIONS SUMMARY

The tradewinds offers conditions that are conducive for duct formation. This arises because of the water vapor content and large scale sinking of dry air, subsidence. Located in the south part of this region, the Amazon has many occurrences not only of surface and elevated ducts, but SRLR as well. Analyzing data from GTE, its possible to find important information for operational use, like seasonality of ducts and SRLR occurrences, as well duct heights.

One possible important factor not considered in the past (climatologic) data, is the diurnal variation of the layer height. This is because the soundings are made at 06:00 and 20:00 LT only.

V. A CASE STUDY OF REFRACTIVE CONDITIONS

Based on previously examined climatologic data relative to abnormal refractive layer occurrences, an examination more suitable for operational evaluations will be made. This examination will consider mean conditions but rather conditions occurring with operational radiosonde profiles from the previously described locations. Further, the profile data will be used as input to propagation models, so the assessments can be made in terms of the effects of the layer, not solely on their occurrence.

A. DATA SOURCE AND PROCESS

The period considered for this case study is between March 06 and June 30, 2003, using records of soundings and satellite imagery. The sounding data analyzed were obtained through a NOAA (National Oceanic and Atmospheric Administration of USA) web site and the satellite photos from NOAA and CPTEC/INPE (Center for Weather Forecast and Climatic Studies / National Institute for Space Research, both in Brazil) sites.

The soundings were used to determine the type, height and thickness of abnormal layers, followed by statistical processes to obtain statistics on significant occurrences. The satellite photos were used to study the relation of abnormal layers with other phenomena, like location of the ITCZ or any specific type of clouds.

Initially the soundings were analyzed through graphs of *M*, *N*, humidity and temperature versus height generated by a Matlab application code, for the purpose of finding trapping layers. As shown previously, a trapping layer is evidenced by negative gradients of *M*, more negative that -157 /km. The trapping layer height, strength and the *M* profile shape, in general, determine the height and thickness of the ducts. These trapping layer values, however, are almost impossible to find graphically when great differences of height are involved, as in this thesis (i.e., 0 to 30000 feet or more). In this case, an alternative method was adopted, through the tactical decision aid (TDA) software in the Advanced Refractive Effects Prediction System (AREPS) version 2.1.

The AREPS and its documentation may be obtained in the Space and Naval Warfare System Center site at http://sunspot.spawar.navy.mil/2858/index.html.

Inserting the sounding data in the FAA604 (WMO/GTS) format directly into AREPS, the program generates a "summary display" that shows the type, height and thickness of abnormal layers. The maximum height considered depends on the available data in the single sounding used. This height may be reduced, if necessary, thus reducing the number of significant levels in the sounding inserted in the AREPS.

The bottom and top heights of the layers may be measured directly in the summary display graphs (*N*, *M* or gradients), and their difference determines the thickness, e.g. the duct or wave-guide thickness. Errors in measurements of approximately 200 ft are expected. The height values used in this thesis are relative to above ground level (AGL) and in feet.

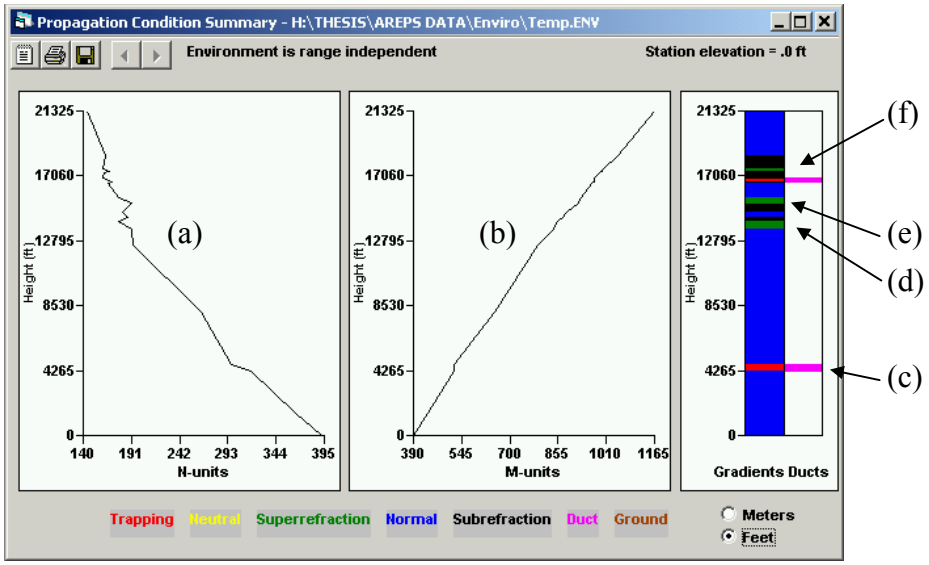

Figure 5.1 – Example of a "summary display" generated by the AREPS about a sounding over Belém in April 08, 2003, at 12:00Z. It is possible to see the (a) *N* profile, (b) *M* profile, (c) a duct at 4450 feet, and three multiple layers composed by: (d) a superrefraction and a subrefraction layers, (e) a subrefraction and superrefraction layers, and (f) a duct, a superrefraction, a subrefraction and a superrefraction layers. Although this sounding has data available up to 48335 feet, the maximum height in this graphic is only up to 21325 feet to show more details.

Single subrefraction, superrefraction and trapping layers (the last one forming ducts) were investigated, as well as multiple layers. The multiple layers studied were made by 18 possible combinations between three different layers, as shown in the Figure 5.2. The maximum number of single or multiple layers considered each day was two. When exceeded, the two highest layers were measured.

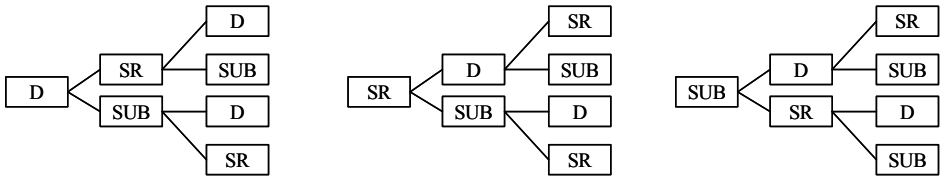

Figure 5.2 – Three single layers and eighteen different multiple layers (2 x 2 and 3 x 3) were analyzed because they affect differently the propagation.

The acronym SR or SRLR is used for superrefraction, SUB for subrefraction and D for ducts. A multiple layer is represented by the sum of layers, for example, SR+SUB means a multiple layer composed by a superrefraction layer with a subrefraction layer on its top. Different combinations of layers affect the propagation differently as will be discussed later.

AREPS allows the simulation of specific system propagation in a specific location (i.e. an airborne radar over Belém) as soon as the sounding data is processed. The type of radar, as well its parameters, may be changed to simulate different operational situations using the same environment.

Two types of radar were used in this thesis: airborne and ground based. Their parameters are listed in the Table 5.1 and represent generic equipment, since the parameters used in the real systems in SIVAM are classified.

In the same way, the ESM system is generic equipment with –70 dBm of sensitivity in the total 1 to 18 GHz of receiving band, using circular polarization. The

target assumed is a small aircraft with a fluctuating radar cross section (RCS). The RCS assumed for 1500 MHz is 3 m^2 and for 3000 MHz, 5 m^2, both for horizontal polarization.

With an objective to limit the number of independent variables, the radar parameters are fixed. The airborne radar was limited to 5775 feet high, because this corresponds to the line-of-sight between the radar and a simulated illicit traffic flying at 500 feet and 120 nmi. In operational situations, the airborne platform must vary its height to improve its endurance, and radar and communications horizon.

Parameters	**Airborne Radar**	**Ground Radar**
Frequency (MHz)	3000	1500
Peak Power (KW)	500	1000
Pulse length (μs)	1	5
Receiver noise figure (dB)	3	5
Assumed system loss (dB)	5	5
Max instrumented range (nmi)	250	250
Probability of false alarm	10E-8	10E-8
Integration of pulses	Incoherent	Coherent
Antenna type	Sin (X)/X	CSC-SQ
Polarization	Horizontal	Horizontal
Hits per scan	16	16
Antenna gain (dBi)	40	38
Horizontal beam width (deg)	1	1.5
Vertical beam width (deg)	1	20
Antenna elevation angle (deg)	-0.8	0.5
Antenna height (ft) AGL	5775	15 to 30

Table 5.1 – Parameters of the generic ground and airborne radars used in this thesis.

B. EFFECTS OF ABNORMAL LAYERS

As discussed in the Chapter III, abnormal refractive conditions may increase or decrease the radar horizon in relation to the horizon with normal refraction. Superrefraction tends to bend the rays downward, more than the normal refraction, following curved earth and, thus, improving radar detection for low-flying targets. If subrefraction occurs, the rays tend to bend upward, decreasing the horizon and low flight detection. In the case of trapping layers and ducts, the detection is greatly increased if the radar and target are inside the duct, but reduced if one of them is outside, since the target would fall into a radar "hole." These first considerations are valid, especially in case of naval radars with one type of layer, and both at sea surface. In the case of radars over land, ground based or airborne, the effects are more complex especially when some combination of layers occurs.

Based on the 354 accepted soundings considered in the Table 5.2, this study analyzed three types of abnormal layers, and, in addition, considered 18 combinations for multiple layers composed of up to three different layers (i.e. a duct right above a superrefraction layer and both right above a subrefraction layer). The criterion used for accepting soundings was the existence of valid measurements of significant levels at 10000 ft minimum. Data from Belém station were available only up to the third day of May.

Station	March	April	May	June	Total/Station
Belém	32	38	3	0	73
Manaus	26	33	41	39	139
Vilhena	19	26	42	55	142
Total/Month	77	97	86	94	354

Table 5.2 – Number of accepted soundings by station during the March-June 2003 period.

Most of the selected soundings had at least one type of abnormal layers. In 354 soundings, 78.8% had one or more abnormal layers, and 21.2% with none. The Table 5.3 compares the number of soundings with or without abnormal layers.

Occurrence	N	%
Only Surface Abnormal Layers	44	12.4
Only Elevated Abnormal Layers	137	38.7
Surface and Elevated Abnormal Layers	98	27.7
Without Abnormal Layers	75	21.2
Total	354	100.0

Table 5.3 – Absolute and relative values about abnormal layers occurrence during the March-June 2003 period.

The occurrence of the abnormal layers, the type and how it affects radars and ESM systems as determined with AREPS simulations, will be discussed in the next sections.

C. ABNORMAL SURFACE AND ELEVATED SURFACE LAYERS OCCURRENCE AND EFFECTS

An interesting and operationally significant result was that neither the surface nor elevated abnormal layers were shown to have significant effects on ground and airborne radars, as well ESM systems. This analysis, however, was made with the purpose of comparing actual with GTE data, as well to formulate the basis of future studies about this subject.

The Table 5.4 shows the occurrence of surface ducts, superrefraction and multiple layers from March to June. There was no occurrence of surface subrefraction layers during this period. The entries show the occurrence in absolute values and percentage relative to the total number of soundings accepted in one month.

It is possible to compare some measured data during the March-June period with the GTE source described in Chapter IV, as shown by Figure 5.3. Surface duct occurrence allows comparisons only for Vilhena station, because this type of occurrence did not happen in the other stations.

Station	Month	Duct		SR		Multiple	
		ABS	%	ABS	%	ABS	%
Belém	March	0	0	3	6.3	0	0
	April	0	0	4	10.5	0	0
	May	0	0	0	0	0	0
	June	0	0	0	0	0	0
Manaus	March	0	0	7	26.9	0	0
	April	0	0	6	18.2	0	0
	May	0	0	4	9.8	0	0
	June	0	0	8	20.5	0	0
Vilhena	March	8	42.1	5	26.3	0	0
	April	12	46.2	4	15.4	0	0
	May	13	31.0	12	28.6	6	14.3
	June	29	52.7	6	10.9	13	23.6

Table 5.4 – Abnormal surface layer occurrence in the March-June 2003 period.

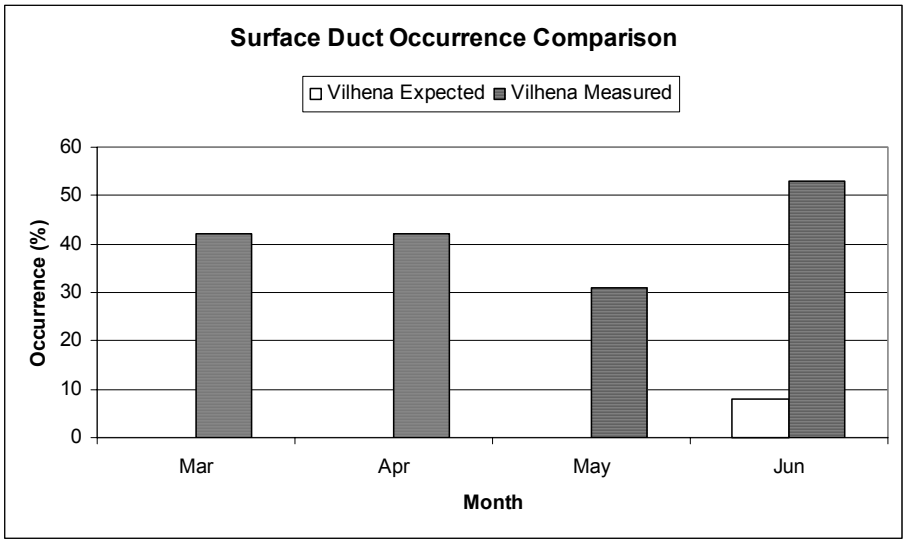

Figure 5.3 – Comparison between expected (GTE) and measured (actual) surface duct occurrence in Vilhena. The other stations did not show this type of ducts during the period studied.

Table 5.5 shows the median height of the surface abnormal layers. The height comparison of surface ducts is shown in the Figure 5.4, again, only for Vilhena.

Station	Month	Median Height (ft)		
		Duct	SRLR	Multiple
Belém	March	0	1350	0
	April	0	1934	0
	May	0	0	0
	June	0	0	0
Manaus	March	0	984	0
	April	0	1646	0
	May	0	1360	0
	June	0	1261	0
Vilhena	March	408	777	0
	April	404	477	0
	May	316	779	610
	June	224	678	446

Table 5.5 – Median height of surface abnormal layers.

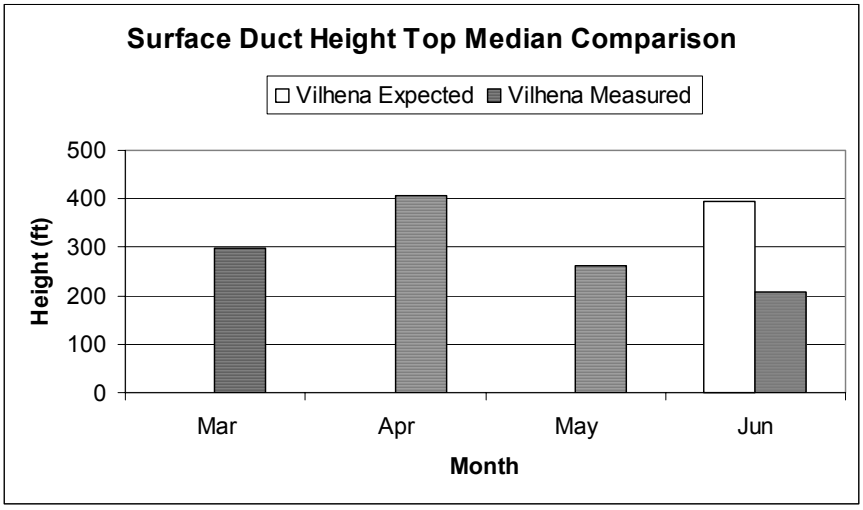

Figure 5.4 – Surface duct height top median comparison between expected (GTE) and measured (actual) data.

Surface superrefraction occurrence, on the other hand, allows better comparisons, as shown by Figure 5.5. Multiple layers were not computed by GTE, but comparisons were made for the purpose of this case study. The type of surface multiple layers and their absolute and relative occurrence in Vilhena are in Table 5.6. Multiple layers, even combining ducts with superrefraction (D+SRLR) or subrefraction layers (D+SUB) at the surface, did not seem to significantly affect the propagation.

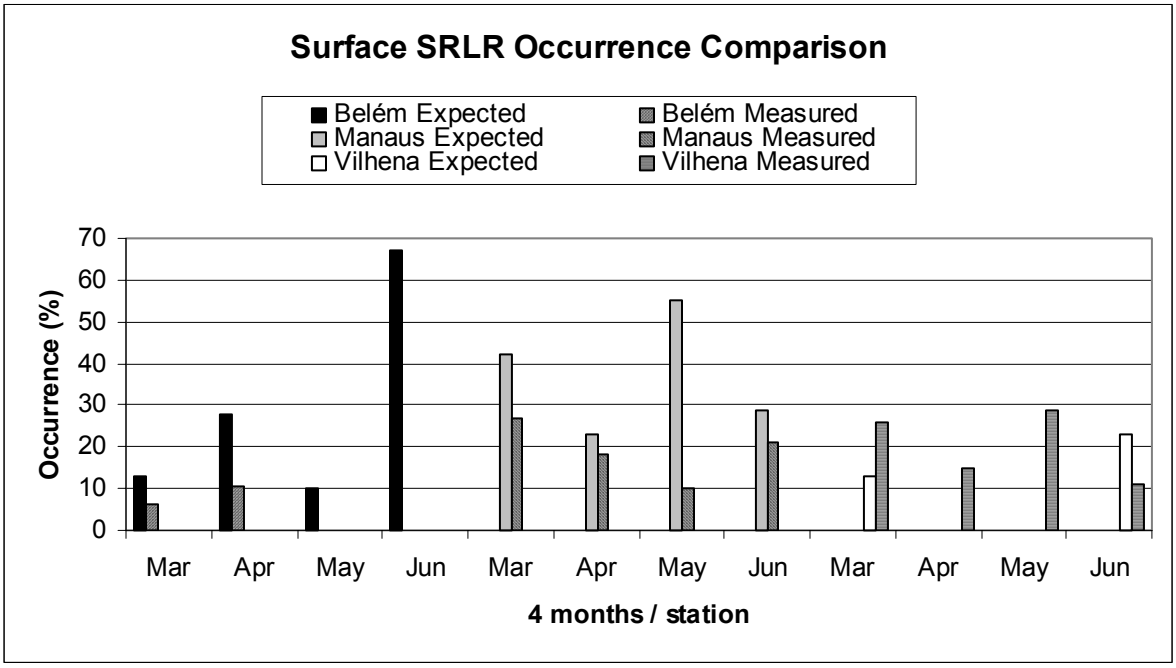

Figure 5.5 – Comparison between expected (GTE) and measured (actual) occurrence of surface SRLR at the three stations.

Month	D+SRLR		D+SUB	
	ABS	%	ABS	%
May	5	12	1	2.4
June	11	20	2	3.6

Table 5.6 – Surface multiple layer occurrence and respective types.

An example of simulation results using AREPS is given in Figure 5.6, generated from a profile at Manaus on 11 April, 2003. It shows the generic ground radar located in

Manaus and its radar coverage in terms of probability of detection (PD) and ESM detection. Although there was surface superrefraction in the Manaus profile on 11 April, no significant effect was noted in the AREPS generated coverage diagram.

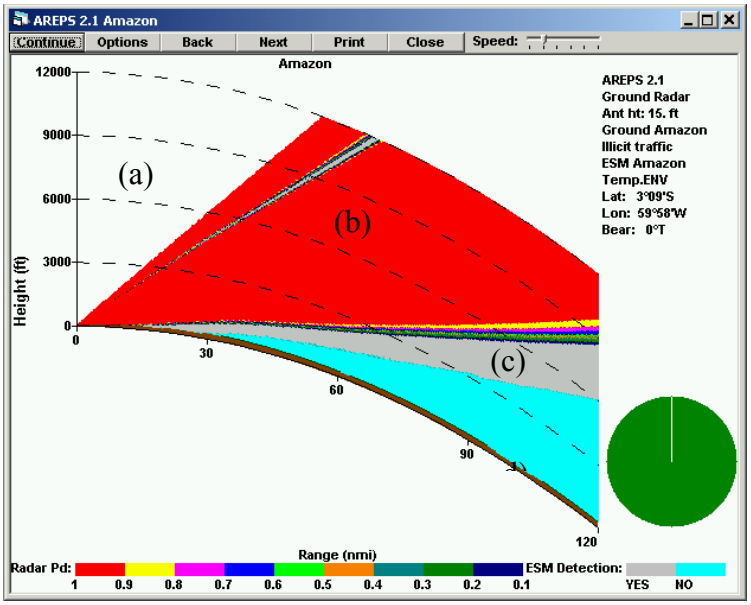

Figure 5.6 – Radar coverage for the generic ground radar located in Manaus, using the sounding of April 11, 2003 at 00:00, when a surface superrefraction layer occurred up to 1820 feet AGL, not affecting significantly the radar propagation. Letter (a) is in the limit of the vertical antenna aperture where there is no detection; in (b) is the region with maximum PD, above 90%; in (c) only ESM detection is possible and in (d) there is no passive or active detection. Surface abnormal layers did not affect significantly the radar coverage in the three stations.

D. ELEVATED LAYER OCCURRENCES AND ITS EFFECTS

While surface-based ducts did not show significant propagation effects for airborne systems, elevated ducts did. Table 5.7 shows the occurrences of elevated ducts, superrefraction, subrefraction and multiple layers during the period analyzed. Any layer with its bottom above 500 feet AGL was considered an elevated layer. The occurrences are shown in absolute values and in percentages, relative to month totals. It is possible to compare some measured data with the GTE. Figure 5.7 shows the comparisons for elevated duct occurrence in the March-June period.

Station	Month	Duct		SRLR		SUB		Multiple	
		ABS	%	ABS	%	ABS	%	ABS	%
Belém	March	7	22	10	31	11	34	1	3
	April	5	13	16	42	20	53	0	0
	May	1	33	0	0	0	0	0	0
	June	0	0	0	0	0	0	0	0
Manaus	March	0	0	6	23	7	27	1	4
	April	0	0	9	27	14	42	4	12
	May	4	1	25	61	26	63	13	32
	June	3	1	12	30	32	82	14	36
Vilhena	March	2	10	3	16	2	10	2	10
	April	5	19	7	27	16	62	4	15
	May	6	14	24	57	22	52	6	14
	June	15	27	33	60	15	27	14	25

Table 5.7 – Elevated abnormal layer occurrence in absolute and relative values.

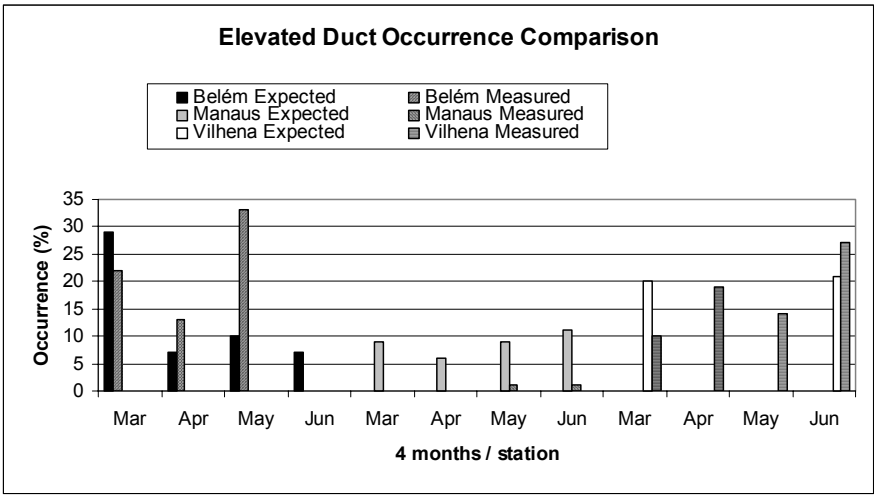

Figure 5.7 – Comparison between expected (GTE) and measured (actual) occurrence of elevated ducts in the three stations.

Although there are some months in the case study without data, it is possible to note that in the months that had data, the elevated duct occurrence did not follow the same behavior predicted by GTE climatologic data. The same can be said about the

height top median, showing different behavior as well, as shown in the Figure 5.8. The mean height, in feet, of each type of layer is shown in Table 5.8.

Station	Month	Median Height (ft)			
		Duct	SRLR	SUB	Multiple
Belém	March	10470	12408	17769	7500
	April	12911	10934	21958	0
	May	0	0	0	0
	June	0	0	0	0
Manaus	March	0	9405	21581	3800
	April	0	7787	23856	16740
	May	9251	11975	20836	14823
	June	4381	11013	20351	16812
Vilhena	March	13260	20154	19740	18638
	April	12419	8923	17738	12928
	May	10791	11028	14693	8138
	June	7105	11131	14364	5922

Table 5.8 – Median height of elevated abnormal layers during the March-June period.

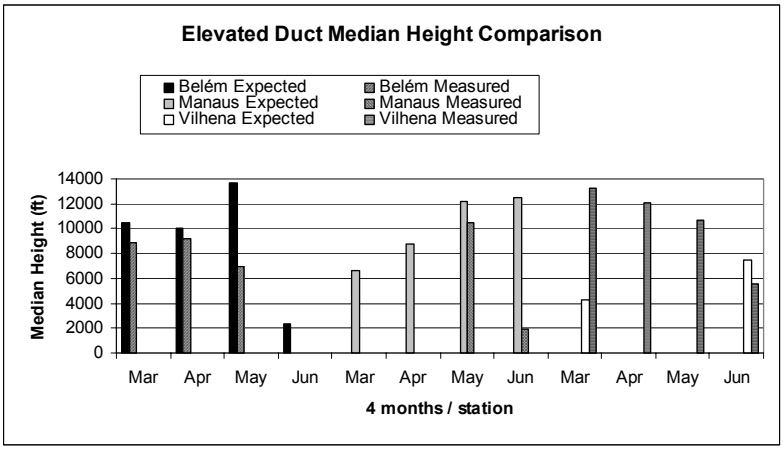

Figure 5.8 – Comparison between expected (GTE) and measured (actual) data about elevated duct height top median.

The occurrence, but not the height, of elevated SRLR computed by GTE and measured data may also be compared, as shown in the graph of the Figure 5.9.

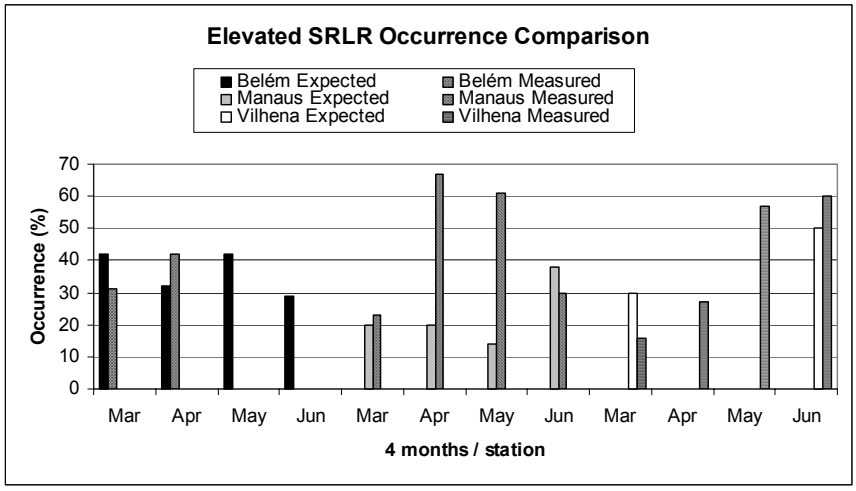

Figure 5.9 - Comparison of elevated SRLR occurrence between GTE and measured data. The measured occurrences did not follow the expected variation.

GTE climatologic data did not include subrefraction and multiple layers, but they were accounted for within this case study because they affect airborne radars, as will be discussed later. The occurrences of multiple layers, designated as such by at least two layers, during the March – June period are shown in the next table. Superrefraction layers with a duct on top (SRLR+D) did not occurred.

More than two different layers in the same multiple layer did not occurred frequently. Three multiple layers like two SUB+SRLR+SUB and one SRLR+SUB+SRLR occurred in Manaus in May (7.6% and 3.8% of occurrence respectively), and one SRLR+SUB+D (5%) in March over Vilhena. Only one multiple layer arising from a sequence of four layers (SRLR+SUB+SRLR+SUB) occurred in June in Manaus (1.8%).

Although the GTE data, as discussed in Chapter IV, identifies only superrefractive layers and ducts, subrefractive layers affect airborne systems as well. When the radar energy is abruptly refracted from its approximate line-of-sight path by an abnormal layer, it causes a sector with decreased, perhaps even no, detection. This

divergence of rays, and hence energy, is caused by an abrupt deviation downwards, upwards or both, as shown in Figure 5.10.

Station	Month	D+SRLR		D+SUB		SR+SUB		SUB+SRLR		SUB+D	
		ABS	%	ABS	%	ABS	%	ABS	%	ABS	%
Belém	March	0	0	0	0	1	3.1	0	0	0	0
	April	0	0	0	0	0	0	0	0	0	0
	May	0	0	0	0	0	0	0	0	0	0
	June	0	0	0	0	0	0	0	0	0	0
Manaus	March	0	0	0	0	1	3.8	0	0	0	0
	April	0	0	0	0	3	9	1	3	0	0
	May	0	0	1	2.4	7	17	2	4.8	0	0
	June	0	0	0	0	0	0	0	0	0	0
Vilhena	March	0	0	0	0	1	5	0	0	0	0
	April	2	7.7	0	0	1	3.8	0	0	0	0
	May	2	4.7	2	4.7	1	2.3	0	0	1	2.3
	June	0	0	0	0	1	1.8	2	3.6	0	0

Table 5.9 – Occurrence of multiple layers consisting of a combination of two different types. The SRLR+D did not occur in the period analyzed.

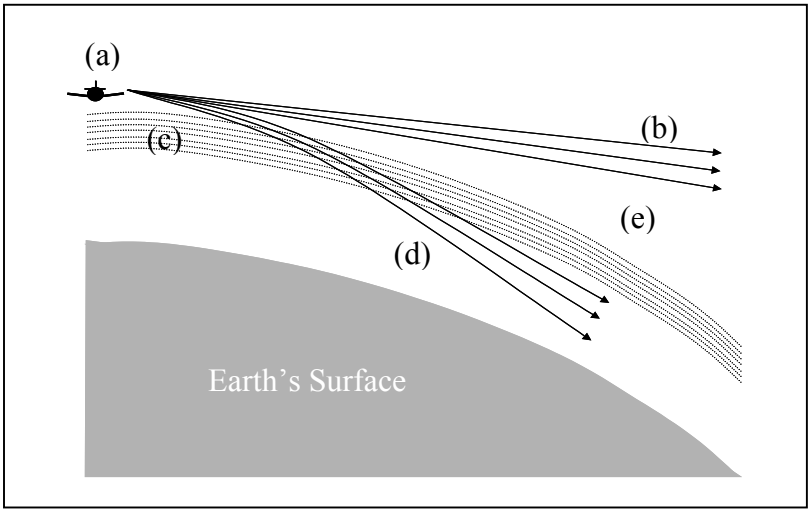

Figure 5.10 – An airborne radar located in (a), with normal refraction, has its rays following a line-of-sight path (b). If an abnormal layer occurs (c), its deviation to other direction (d) causes a sector with reduced or no detection (e). The rays are refracted downwards or upwards depending on the type of the abnormal layer.

The rays' deviation, and consequently the sector with low detection, varies with the gradient of the refraction index (the strength of the layer), angle of incidence of the radar energy in the layer, and radar parameters, like power, frequency and antenna gain. In this thesis, however, the radar parameters were fixed, as well its height, at 5775 feet AGL.

If no abnormal layers occur, the coverage over Manaus for the airborne radar and ESM systems would be as shown in the Figure 5.11. In this graphic representation, it is possible to see the radar energy distributed by its entire antenna vertical aperture, with few ground reflections. Outside this region the PD is lower than 50%. Below 0% of radar PD, only ESM detection is possible, up to its range limit.

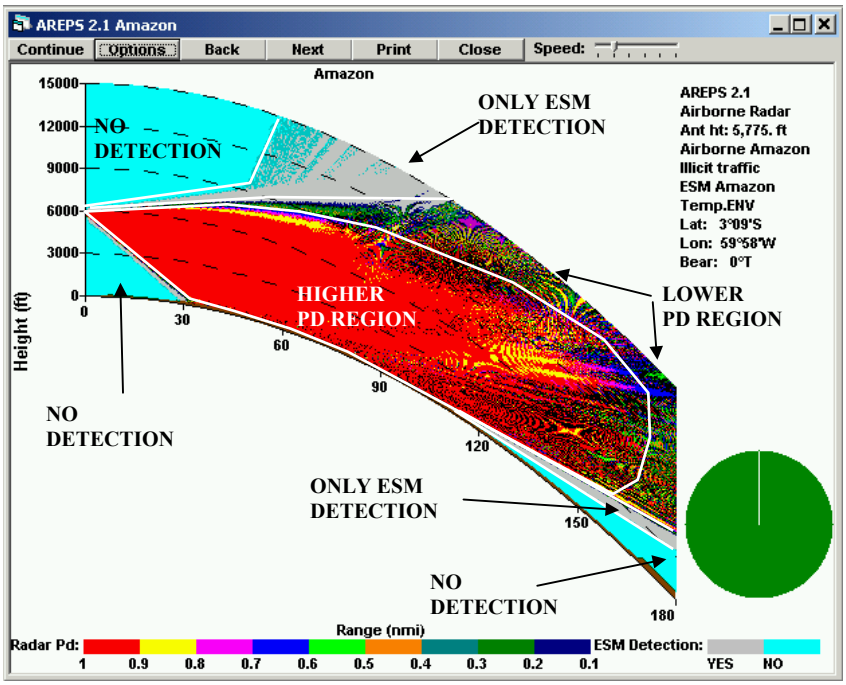

Figure 5.11 – Regions of active and passive detection for the airborne radar generated by AREPS, based in a sounding without abnormal layers over Manaus. White lines where added to show details. ESM detection occurs always in the regions below and above the radar coverage.

The radar and ESM coverage is changed with the presence of abnormal layers. The Figure 5.12 shows the effect of a superrefraction layer between 4450 and 5050 feet over Manaus three days later, in April, 16 2003, at 12:00Z. In this Figure it is possible to note that although at 120 nmi the simulated illicit traffic at 500 feet should be detected, the PD between 6000 and 12000 feet was reduced to below 50%.

As occurred in other simulations, the height where the energy starts its deviation is always at the top of the superrefractive layer, 5050 feet in this case. Above this, the energy followed its direct path, where no other abnormal layer occurred. The distance from the radar where this deviation occurs changes with the variables described before, like radar power, frequency or angle of incidence. The knowledge about the height and distance, that is, where the energy divergence occurs and "holes" form, is important for operational use.

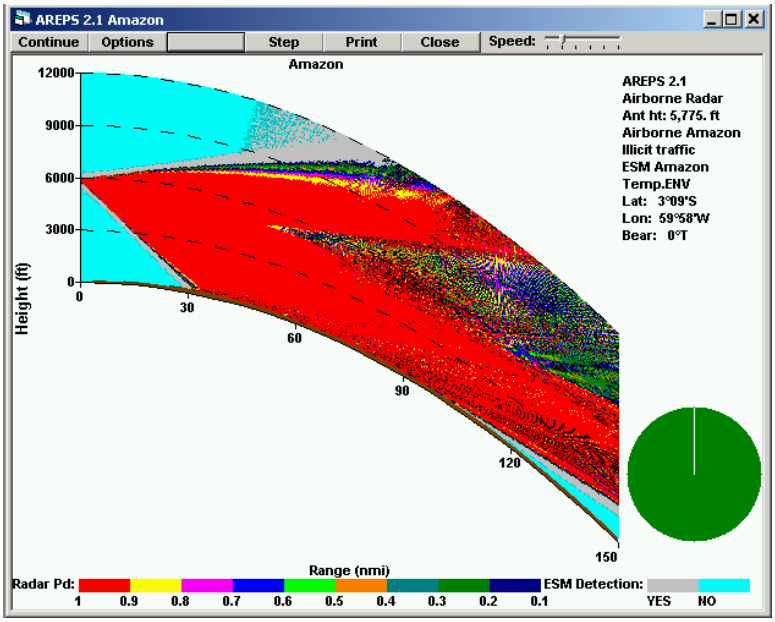

Figure 5.12 – A superrefraction layer between 4450 and 5050 AGL over Manaus caused the divergence in the radar coverage, creating a sector with lower PD. The energy divergence starts at the top of the layer.

Subrefraction layers may cause similar effects, as illustrated by the example in the Figure 5.13, where a sector with decreased probability of detection appears. This layer occurred above Manaus on May 23, 2003, at 00:00 Z, between 5620 and 6700 feet. Again, the low flight detection was not affected, but at about 120 nmi the probability of detection decreased to below 50% between 6000 and 12000 feet. The height where the radar energy started its divergence was approximately 5600 feet, the bottom of the subrefraction layer.

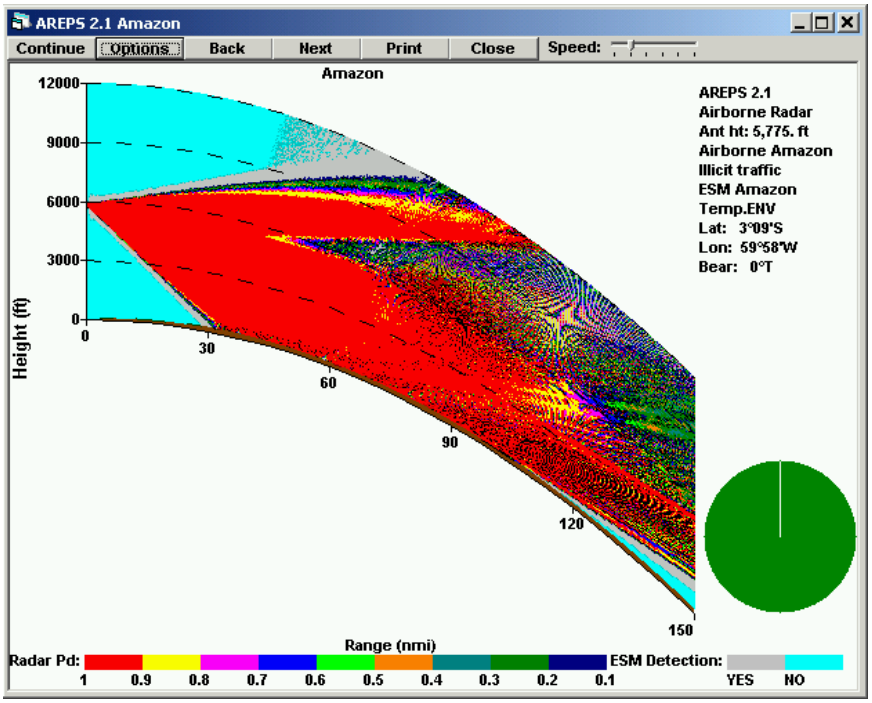

Figure 5.13 – Subrefraction layers may cause the splitting of the radar energy, as a superrefraction does, but, in this case, the deviation of the path starts in the bottom of the layer.

Some types of multiple layer combinations are conducive to forming radar "holes." This is very important in airborne C4I operations, i.e. airborne control platforms such as the EMB-145. For example, if a superrefraction layer with a subrefraction on top (SRLR+SUB) occurs, its lower part tends to refract the rays downward, while the upper part, bends rays upward. It forces the energy to divide itself in two different directions. One example is shown in the Figure 5.14, occurred above Manaus in March 08, 2003 at 00:00 Z. Superrefraction between 1360 and 3000 feet, combined with subrefraction from 3000 to 3800 feet, form this multiple layer.

It is noted that the energy divergence occurs at 3000 feet, where the change between superrefractive and subrefractive layers occurs. At 120 nmi the detection of low flying targets was strengthened because the energy was refracted to, or converged, at this lower region. At the same time, a sector with lower probability of detection (70-60% and less) was formed between 2000 and 6500 feet. In the upper part of this sector the

detection was strengthened again, as a result of the upward deviation caused by the subrefraction layer. A subrefraction layer on top of a duct tends to cause the same effect, but stronger, as will be shown.

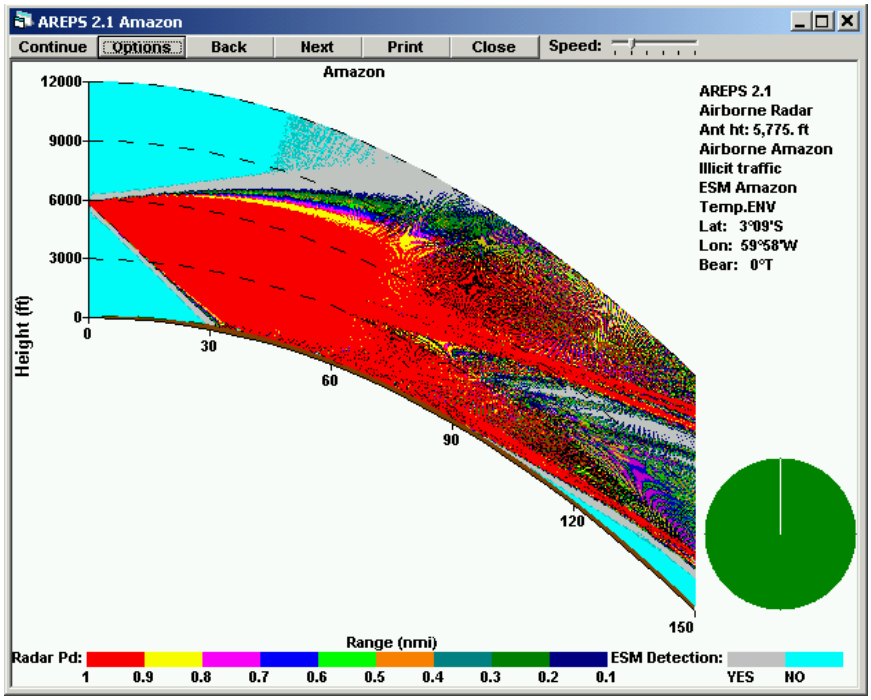

Figure 5.14 – Some combinations of layers, as a superrefractive layer with a subrefractive on top, help the radar propagation splitting.

Some types of multiple layers, on the other hand, tend to avoid the formation of a well-defined sector with lower or no detection. One example is shown by the Figure 5.15, where a multiple layer composed of two alternate superrefraction and subrefraction layers (SRLR+SUB+SRLR+SUB) caused multiple paths to the target from the radar. This multiple layer occurred over Manaus between 919 and 3983 feet on June 30, 2003 at 12:00Z.

As shown in the Figure 5.15, the energy diverges two times; one at approximately 1700 feet and other at 3400 feet high. These two altitudes occurred at the intersections between the superrefraction and subrefraction layers. In this case, a well-defined sector with lower PD was the outcome.

Ducts are the primary atmospheric phenomenon that refracts the radar energy from its direct path, creating sectors with lower PD immediately above the duct, as shown by the example in the Figure 5.16.

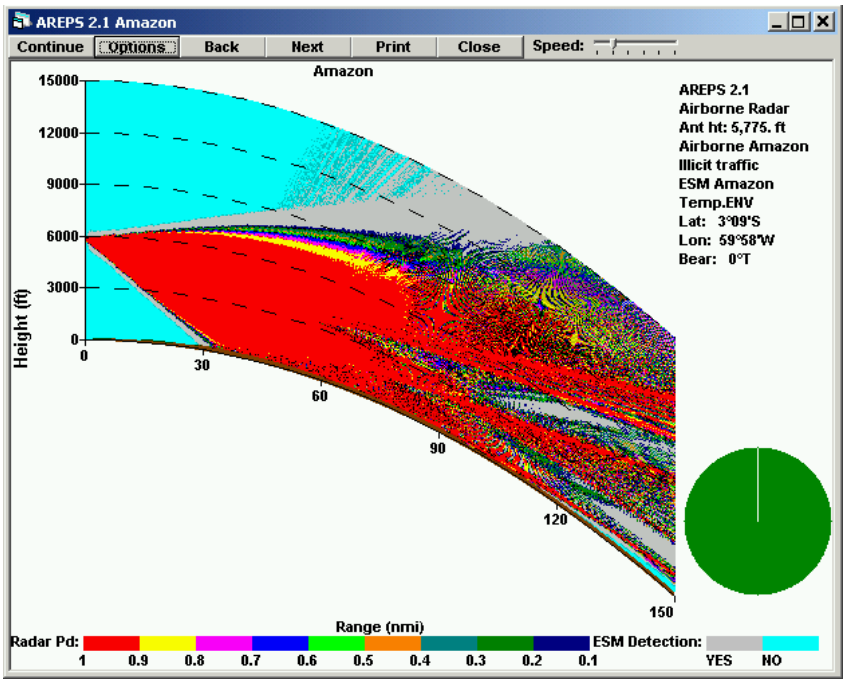

Figure 5.15 – Some combinations of layers tend to spread the radar energy, as a subrefractive layer with a superrefractive on top.

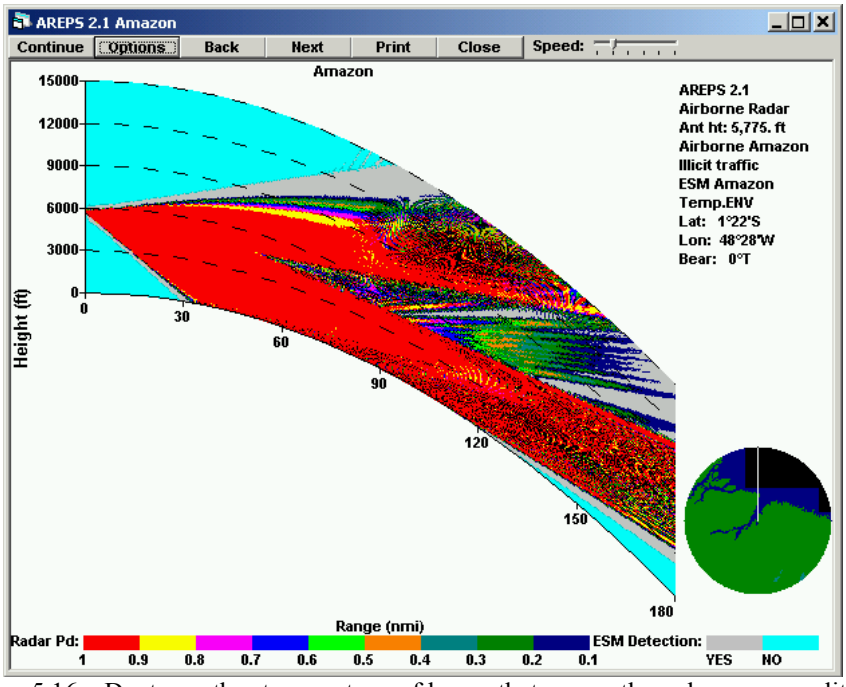

Figure 5.16 – Ducts are the stronger type of layers that causes the radar energy splitting.

This duct, caused by an elevated trapping layer, occurred over Belém on April 08, 2003 at 12:00Z between 4250 and 4700 feet AGL. The energy diverges on the top of the duct. At 120 nmi the detection at lower altitudes was improved, but higher, a sector with lower PD was formed between 5000 and 9000 feet. If the radar and the duct were higher, the effect should be stronger, because ground reflections would not be present.

Duct effects may be even stronger if the duct is combined in a multiple layer, like a duct with a subrefraction layer on top (D+SUB). While the duct strongly refracts or deviates the radar energy downwards, the subrefraction layer refracts it upwards. An example is shown in the Figure 5.17, using a Belém's sounding of March 15, 2003, at 12:00Z. A duct was formed between 4215 and 5550 feet, followed by a subrefraction layer up to 6900 feet. The energy splits, again, on the top of the duct.

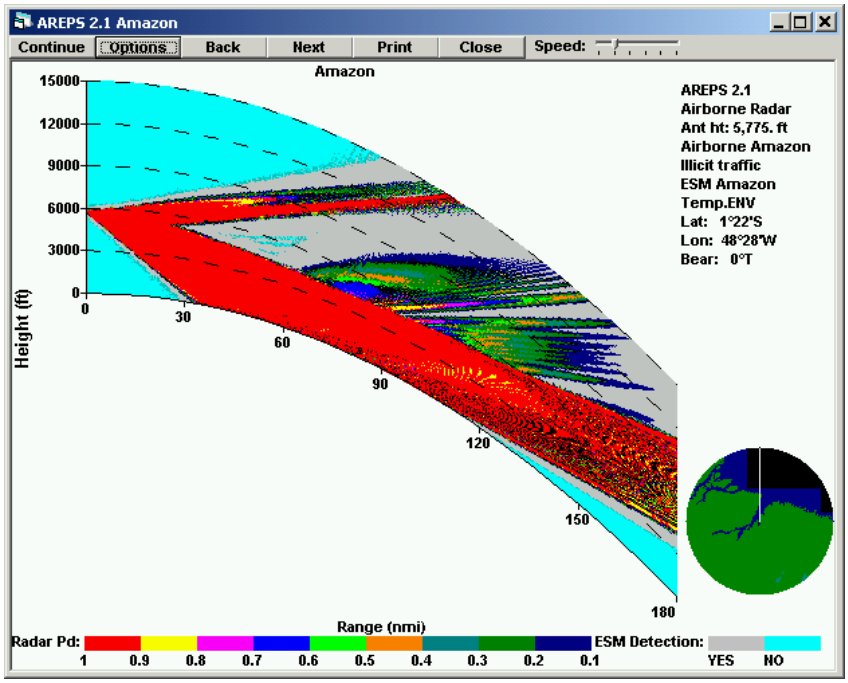

Figure 5.17 - Duct effects may be even stronger if the duct is combined in a multiple layer where one refracts the radar energy downwards and other upwards, like a duct with a subrefraction layer on top.

If the sequence of this multiple layer were inverted (a subrefraction layer with a duct on top), its effects should be weaker, because the subrefraction layer would refract the energy and overcome the "hole" created above the duct. A similar effect is expected

to happen with a superrefraction and subrefraction layers (SR+SUB). As these types of multiple layers occurred in higher altitudes and did not affect the radar at 5775 feet, a specific example will not be shown.

E. STABILITY OF ABNORMAL LAYERS

Another important consideration is how long these abnormal layers stay over their stations. An analysis of this, however, presents special difficulties since there are some gaps in the sounding sequence (days without data) and the layers also change height and intensity with time. For example, in three soundings the same superrefraction layer may become trapping, then again, superrefractive, with few changes in its refractive index. Additionally, some layers apparently combine with other forming multiple layers, which may divide again into single layers by the next sounding.

The criteria adopted for counting the occurrences were the existence of a similar layer in a single sounding, and its repetition each 24 hours, even if combined in a multiple layer. The allowed height variation in 24 hours was 5000 feet for layers below 20000 feet, and 10000 feet of variation for layers above. Table 5.10 shows how long each type of abnormal layer persisted above its station during the study. The period without any abnormal layers was included as well. This table indicates that, for example, in Belém, 85% of the superrefraction layers existed only one day, while 15% for two days; 90% of the days were without any elevated abnormal layer for a one-day period, while 10%, for two days.

One special situation occurred in Vilhena between June 08 and 22, when a superrefraction layer alternated with ducts persisted without interruption between 4500 and 9200 AGL. During these 14 days, the region over Vilhena, in a radius of approximately 400 nmi, had light or no clouds. One example is the image from GOES-12 (CPTEC/INPE) in June 17, 2003, at 21:00Z, shown by the Figure 5.18. This type of satellite image was chosen because it shows different colors for different temperatures, which help to estimate the cloud height.

Station	Layer Type	Duration of elevated layers							
		1 day		2 days		3 days		4 days	
		ABS	%	ABS	%	ABS	%	ABS	%
Belém	Duct	10	100	0	0	0	0	0	0
	Superrefraction	11	85	2	15	0	0	0	0
	Subrefraction	3	100	0	0	0	0	0	0
	None	10	90	1	10	0	0	0	0
Manaus	Duct	7	78	2	22	0	0	0	0
	Superrefraction	33	89	4	11	0	0	0	0
	Subrefraction	26	81	6	19	0	0	0	0
	None	3	75	1	25	0	0	0	0
Vilhena	Duct	15	51	0	0	0	0	0	0
	Superrefraction	14	78	2	11	1	5.5	1	5.5
	Subrefraction	22	88	2	8	1	4	0	0
	None	9	100	0	0	0	0	0	0

Table 5.10 – Duration of elevated abnormal layers.

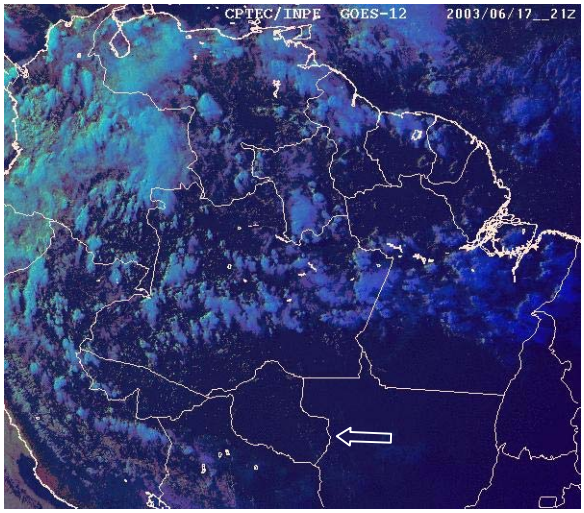

Figure 5.18 – Image from satellite GOES-12 showing the area over and around Vilhena with no clouds in June 17, 2003 at 21:00Z. Vilhena had persistent superrefraction layers alternated with ducts during June 08 and 22. The arrow in south of the map marks its position. (From: http://www2.cptec.inpe.br/satelite/metsat/imagset/az_c.jpg).

Satellite images taken during the case study period could show some evidence about abnormal layers in the Amazon. This is an important consideration because the region is data sparse, except for the three stations used and a few others. Satellite imagery, however, describes the whole basin even though it is from a satellite borne sensor that detects only horizontal variations. Horizontal images that show clouds are valuable because vertical properties can be inferred from satellite sensed cloud properties. For example, convection cloud regions can be expected to be void of layers.

In contrast, when the same region had no elevated abnormal layers, the satellite images showed the presence of convective clouds, as shown in the Figure 5.19.

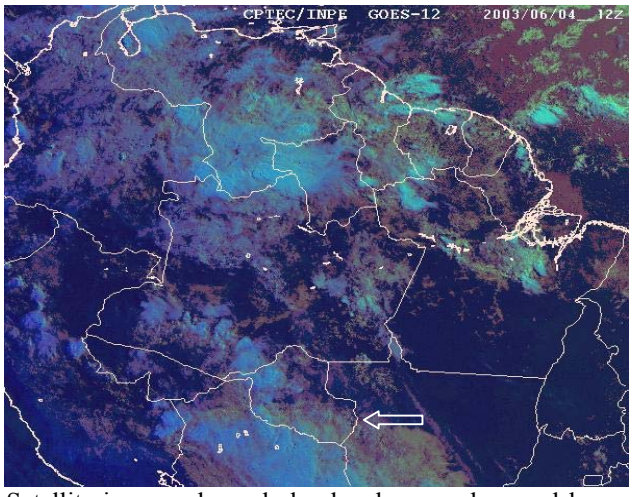

Figure 5.19 – Satellite images showed clouds when no abnormal layers occurred in the Vilhena, marked by the arrow. (From: http://www2.cptec.inpe.br/satelite/metsat/imagset/az_c.jpg).

A similar situation may be observed in Manaus, as shown in the Figure 5.20. In a shorter period, May 12 through 15, this station had four days of alternating superrefraction layers and ducts, between 12000 and 14000 feet. At the end of this period, the satellite image of May 16 at 12:00Z showed Manaus covered by clouds, especially at lower levels, as shown in the Figure 5.21. Belém station did not have sufficient available data for this type of analysis.

Although superrefraction layers and ducts are associated with no clouds days, subrefractive layers seem to be related with higher clouds. Unfortunately, the relatively

short period of satellite images available did not make it possible to establish a strong relationship between occurrences of abnormal layers with clouds using satellite images. A similar situation happened with the study about the relationship between the ITCZ position and layer occurrence. This limited examination, however, certainly suggests that such a study is warranted.

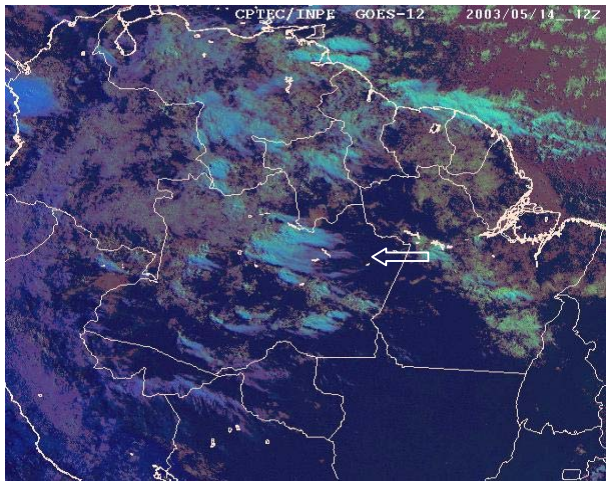

Figure 5.20 - During a period of four days Manaus region presented few clouds and occurrence of stable superrefraction layers and ducts between 12000 and 14000 feet. The clouds at W - NW of Manaus are in higher levels. Manaus is located in the arrow in the center of the map. (From: http://www2.cptec.inpe.br/satelite/metsat/imagset/az_c.jpg).

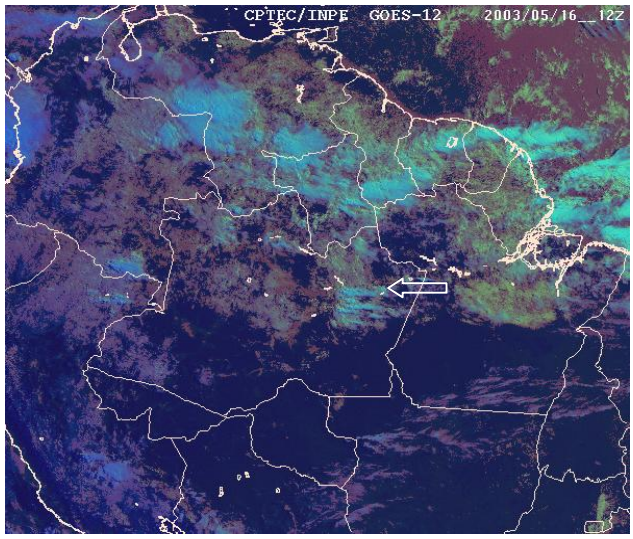

Figure 5.21 - In May 16 2003 there were not abnormal layers above Manaus, which was covered by lower level clouds. (From: http://www2.cptec.inpe.br/satelite/metsat/imagset/az_c.jpg).

The ITCZ could be followed using NOAA data from satellite imagery in the same short period. Figure 5.22 shows the initial position of the ITCZ in May 09. At the end of June, the ITCZ moved to North, reaching the position shown by the Figure 5.23. This movement is related to the natural changing of the ITCZ following the summer hemisphere.

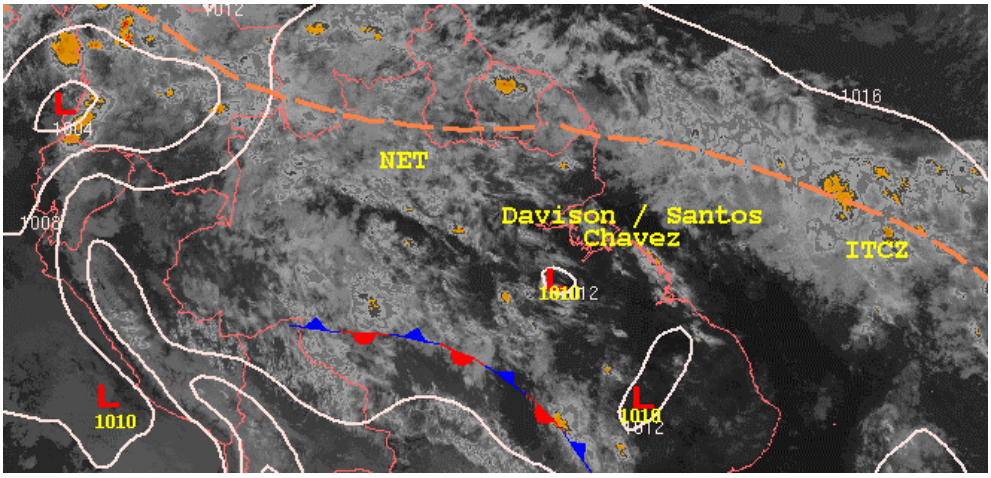

Figure 5.22 – ITCZ position in May 09, at North of Brazil. (After: http://www.hpc.ncep.noaa.gov/international/sampssfc00sat.gif)

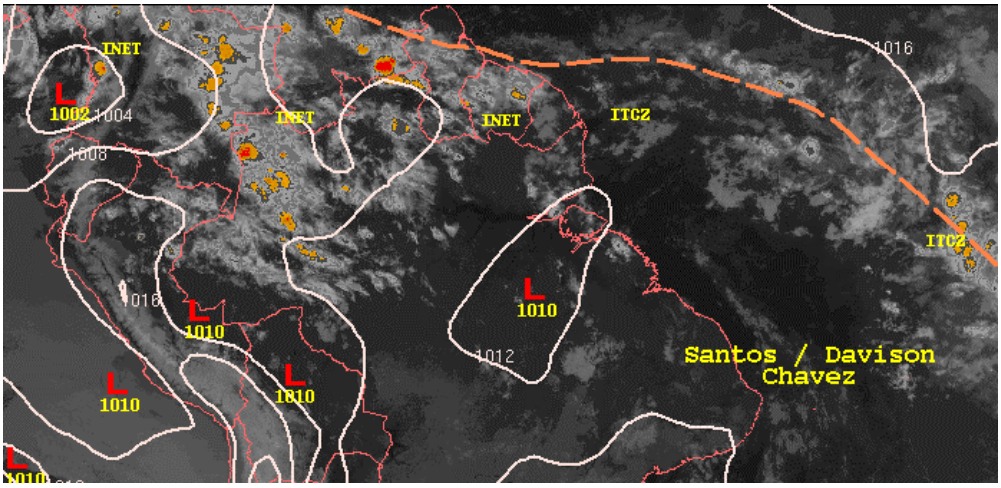

Figure 5.23 – ITCZ position in June 30. Between May and June, the ITCZ moved in the North direction. (After: http://www.hpc.ncep.noaa.gov/international/sampssfc00sat.gif)

Again, because of the relatively small number of satellite images available, it was not possible to establish a strong relationship between occurrence of abnormal layers and the ITCZ position.

F. CASE STUDY SUMMARY

This chapter described the analysis of 354 soundings in the Belém, Manaus and Vilhena stations using the AREPS 2.1 software. In most of soundings it is possible to find one or more abnormal layers that, depending of the type, have specific effects on the radar propagation. These effects were described on the basis of simulated airborne radar operating within elevated abnormal layers, since in other situations there are no significant effects.

Basically, when the radar energy is refracted upwards or downwards, a sector or "hole" with reduced or no detection is created. This reduces the radar detection in that region but the ESM detection is maintained. The height where the radar energy diverges due to refractive effects is related to the bottom of a subrefractive layer or to the top of a superrefractive layer. The type and sequence of multiple layers affect the intensity of this sector with lower PD. Most of the abnormal layers persisted one day long.

Satellite images may be useful to show special conditions when abnormal layers occur, but it is necessary that a larger quantity of data be examined to establish a relationship between them.

VI. CONCLUSIONS AND RECOMMENDATIONS

The Brazilian Government uses active and passive electronic systems for protection and development of the Amazon region, which represents 60% of its territory. The performance of these systems depends on electromagnetic propagation, which is affected by atmospheric refraction. In the troposphere, where significant variations from standard of pressure, temperature and humidity occur with height, layers are formed with different refractive indices. In the Amazon, high water vapor and large-scale vertical motion within the weather patterns form these abnormal refractive layers. Advection and subsidence of relatively dry air aloft cause overlying air to differ from the high water vapor content atmosphere below.

The occurrence of refractive layers was examined on the basis of climatologic data. A case study was performed of abnormal refractive layer occurrence in Amazon environment during the March-June 2003 period, and how it affects the electromagnetic propagation for radar and ESM systems. Open sources were used to obtain software for computer simulations, satellite imagery and soundings about three stations in that region.

The abnormal layer occurrence may be considered high, as showed by 78.8% of the soundings having one or more of them. Surface layers did not show significant effects in simulations using generic radars and ESM. However, elevated layers did, for elevated transmitters. They occurred in 66.4% of the total soundings analyzed and significantly affected airborne systems. Basically, the electromagnetic energy from an airborne radar divergences because of the abnormal layer, creating a sector aloft with low, or even no detection, i.e. a radar coverage “hole.”

In 15.5% of the total soundings used in this case study, superrefractive and subrefractive layers form adjacent elevated multiple layers that, depending on the arrangement, vary the effects from stronger to weaker. However, an important observation was that in the sectors where the active detection was decreased or lost, the passive detection seemed to be unaffected, i.e. was the same as it would be without the abnormal layers.

The knowledge about the conditions that promotes the radar energy divergence or "holes," as well the height and distance where it occurs are important information for operational use. A platform with airborne radar was shown to benefit from operations that avoid gaps in its coverage by choosing its altitude on the basis of refractive layer positions. Simulations showed that the coverage gaps/hole occurrence starts at the height of a superrefractive layer top or at the subrefractive layer bottom.

Because the climatological and case studies showed refractive layers to be significant features of the Brazilian Amazon region, there is concern about the adequacy of real time information on the responsible features. As the Brazilian Amazon is about 5,000,000 km^2 and the atmospheric conditions measurements (i.e. using a balloon) are valid for a limited area and time over the surface, an efficient operation of airborne systems will clearly need more information than those actually available at Amazon meteorological stations. However, although a bigger number of stations and more frequent soundings give more information, airborne radars may be used in areas without meteorological data. Therefore, it is recommended that its platform have some system to do these measurements.

Even with vertical limitations, a refractometer, or some kind of expandable sensor as used in balloons or rockets, launched downwards by gravity, should provide important information about an area of interest. This information should be analyzed in real-time by software like the AREPS.

Finally, this thesis represents one of the first to approach, using recent propagation modeling technology, the study of abnormal layer occurrence in the Brazilian Amazon and its influence on electromagnetic propagation for radar and ESM systems. Although it is possible to reach some conclusions about this topic, it is necessary to conduct a more comprehensive study in time and area to establish more reliable forecasting about these conditions and effects.

APPENDIX A

LIST OF ACRONYMS

AGL.....Above Ground Level

AREPS.....Advanced Refractive Effects Prediction System

ATC.....Air Traffic Control

CPTEC.....Center for Weather Forecast and Climate Studies (Brazil)

CSC-SQ.....Cosecant Squared

D.....Duct

EM.....Electromagnetic

ESM.....Electronic Support Measures

GMT.....Greenwich Mean Time

GTE.....Global Tropospheric Experiment

GTS.....Global Telecommunication System

IFF.....Identification Friend or Foe

INPE.....National Institute for Spatial Research (Brazil)

ITCZ.....Intertropical Convergence Zone

LT.....Local Time

MSL.....Mean Sea Level

NOAA.....National Oceanic & Atmospheric Administration

OTHR.....Over the Horizon Radar

PD.....Probability of Detection

RCS.....Radar Cross Section

SATCOM.....Satellite Communication

SIPAM.....System for the Protection of the Amazon

SIVAM.....System of Vigilance of Amazon

SPSS.....Statistical Package for Social Sciences

SRLR.....Superrefraction Layer

SUB.....Subrefraction Layer

WMO.....World Meteorological Organization

LIST OF REFERENCES

Aviation Today. *SIVAM: Communication, Navigation and Surveillance for the Amazon*. Avionics Magazine of June 2002, from: http://www.aviationtoday.com/reports/avionics/previous/0602/0602sivam.htm, accessed in April 21, 2003 at 23:18.

Batista, N. N. M., Calbete, E., Machado, L. H. R., Oliveira, G. S., & Quadro, M. F. L. *Precipitation and Temperature Climatology*. From: http://www.mct.gov.br/clima/ingles/comunic_old/cinpe02.htm accessed in June 09, 2003 at 22:05.

Davidson, Kenneth L. *Assessment of Atmospheric Factors in EM/EO Propagation.* Course Notes, Department of Meteorology, Naval Postgraduate School, Monterey, California, January 2003.

Fisch, G., Marengo, J. A., & Nobre, C. A. *Climate in Amazonia*. From: http://www.mct.gov.br/clima/ingles/comunic_old/cinpe03.htm accessed in June 09, 2003 at 22:11.

Lutgens, Frederick K., & Tarbuck, Edward J. *The Atmosphere*. Englewood Cliffs, New Jersey, Prentice-Hall, 1982, 2 ed., Ch. 14.

Martin, C. L., Fitzgerald, D., Garstang, M., Oliveira, A. P., Greco, S., & Browell, E., *Structure and Growth of the Mixing Layer Over the Amazonian Rain Forest,* Journal of Geophysical Research, Vol. 93, No. D2, Feb. 20, 1988.

NAVEDTRA 172-10-00-83. *Introduction to Wave Propagation Transmission Lines , and Antennas*. NEETS module 10, Washington, D.C., Government Printing Office, USA, 1983.

Ortenburguer, L. N., Lawson, S. B., & Paterson, B. J. *Radiosonde Data Analysis IV*. Monthly Statistics Report, Tropospheric Ducting Parameters Values, Vol III. Mountain View, CA, Western Division, GTE Government Systems Corporation, 1985.

Raytheon (2002). *The Amazon, which has nearly one third of the entire area of the world's tropical rain forests, is essential for the climate and biological diversity of the planet Earth***.** From: http://www.raytheon.com/products/sivam/sub3.html, accessed in August 27, 2003 at 10:30.

Ringwalt, D. L., MacDonald, F. C., *Elevated Duct Propagation in the Tradewinds*, IRE Trans. on Antenna and Prop., AP-9, July 1961.

Skolnik, Merrill I., *Introduction to Radar Systems,* 3rd ed., McGraw Hill, New York, NY, 2001.

ThinkQuest (1998) Team 20248. *Amazon Life*. *Learning ecology through Amazon rain forest*. From: http://library.thinkquest.org/20248/hid.html accessed in June 24, 2003 at 10:45.

INITIAL DISTRIBUTION LIST

1. Defense Technical Information Center
   Ft. Belvoir, Virginia

2. Dudley Knox Library
   Naval Postgraduate School
   Monterey, California

3. Professor K. L. Davidson
   Meteorology Department
   Naval Postgraduate School
   Monterey, California

4. Professor D. C. Jenn
   Department of Electrical & Computer Engineering
   Naval Postgraduate School
   Monterey, CA

5. Professor D. C. Boger
   Department of Information Sciences
   Naval Postgraduate School
   Monterey, CA

6. Commander
   Comando-Geral do Ar
   Brasilia, DF, Brazil
   Attn: Chefe do CGEGAR

7. Dr. José Edimar Barbosa
   Aeronautical Institute of Technology (ITA)
   Divisão de Engenharia Eletrônica - IEEE
   São José dos Campos, SP, Brazil